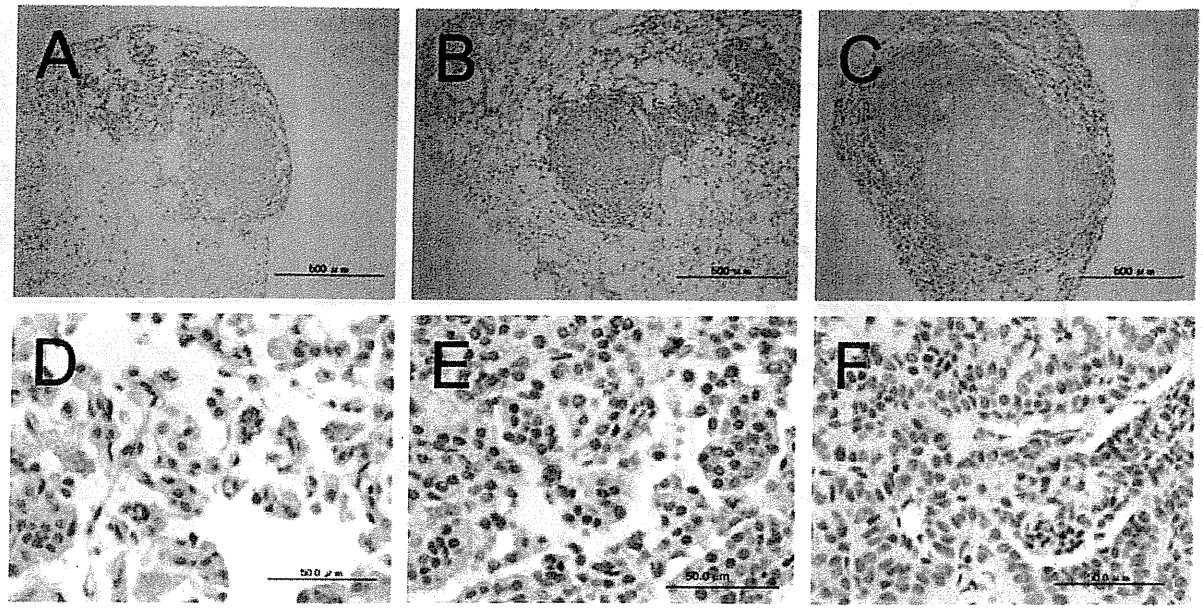


Figure 4. *Immunohistochemical findings for lung space occupied lesion (SOL) developed by urethane treatment. Immunohistochemical analysis of cyclooxygenase-2 (COX-2) (A-C) and vascular endothelial growth factor (VEGF) (D-F) expression in lung hyperplasia (A, D), adenoma (B, E) and adenocarcinoma (C, F) was performed using serial sections of the sample shown in Figure 3, respectively. Bar: 500 μm for A-C and 50 μm for D-F.*

Table III. *Size of lung SOLs at 26 weeks, assessed by micro-CT and by digital caliper.*

| Indomethacin | | Diameter (mm) | | | | |
|---|---|---|---|---|---|---|
| | | Hyperplasias | Adenomas (Ad) | Adenocarcinomas (Ca) | Total SOLs | Ad+Ca |
| 0 ppm | Micro-CT | 1.52±0.37 | 1.82±0.55 | 2.03±0.33 | 1.74±0.51 | 1.85±0.53 |
| | Digital Caliper | 1.42±0.55 | 1.79±0.56 | 1.94±0.65 | 1.65±0.60 | 1.81±0.58 |
| 5 ppm | Micro-CT | 1.33±0.40 | 1.49±0.41 ** | 2.93 | 1.45±0.44 ** | 1.52±0.46** |
| | Digital Caliper | 1.30±0.49 | 1.52±0.43* | 2.65 | 1.46±0.48* | 1.54±0.45* |

Data are mean±SD. **$p<0.01$ *vs.* 0 ppm. *$p<0.05$ *vs.* 0 ppm.

decrease after 18 weeks, and indomethacin suppressed lung SOL development effectively at that period. Of note, one adenocarcinoma observed in the indomethacin-treated group, which was diagnosed at the end of experiment, existed as an SOL in CT images from 10 weeks.

*Size of lung SOLs assessed by micro-CT.* The longitudinal diameters of lung SOLs at 26 weeks, assessed by micro-CT, were similar to those measured by digital caliper after sacrifice (Table III). The longitudinal diameter tended to increase with histological changes, *i.e.* hyperplasia to adenocarcinoma. Indomethacin treatment reduced the size of lung tumors, especially of adenomas (Table III).

Figure 2A shows growth curves for all nine adenocarcinomas developed in A/J mice with or without indomethacin treatment. The adenocarcinoma grew most aggressively, 0.19 mm in diameter in one week (line no.1), and appeared as solid-type nodules with a clear tumor margin on micro-CT images (Figure 2B). Histopathologically, images exhibited an irregular nodular growth pattern without any glandular or tubular formation with little connective tissue. Nuclei were pleomorphic and mitotic figures were also observed (Figure 2D). Representative micro-CT images of hyperplasia, adenoma and other adenocarcinoma (line no.3 of Figure 2A) developed in A/J mice without indomethacin treatment, are shown in Figure 3. On the other hand, hyperplasia and adenoma grew at a slow to moderate speed throughout the experiment. These hyperplasias (Figure 3A) and adenomas (Figures 3B) exhibited clear edges and/or spiked edges in CT images. Figure 3B illustrates a papillary-type adenoma. As seen in adenoma, mitotic rates and degree of cellular pleomorphism were low. One adenocarcinoma

Table IV. *Number of lung SOLs grown more than twice in diameter in A/J mice assessed by micro-CT.*

| Indomethacin | Hyperplasias | Adenomas (Ad) | Adenocarcinomas (Ca) | Total SOLs | Ad+Ca |
|---|---|---|---|---|---|
| 0 ppm | 12 (33) | 32 (49) | 8 (8) | 52 (90) | 31 (58) |
| 5 ppm | 10 (26) | 18 (48)* | 1 (1) | 29 (75)* | 18 (44) |

Numbers in parentheses are total lung SOL numbers. *$p<0.05$ *vs.* 0 ppm.

(Figure 2A, red line, no.2), developed in the indomethacin-treated group was a large tumor that grew particularly rapidly, increasing from 0.9 mm to 2.9 mm within 16 weeks. This solid-type nodule with a clear tumor margin on CT images, is illustrated in Figure 2C.

The number of tumors that doubled in size from first detection was significantly reduced upon indomethacin treatment (Table IV). Regardless of indomethacin treatment, all adenocarcinomas more than doubled in diameter.

*Expression of COX-2 and VEGF in lung SOLs.* COX-2 immunostaining was performed to confirm the existence of molecules targeted by indomethacin (Figures 4A-C). The data were obtained from serial sections used for Figure 3. COX-2 was up-regulated in eight examined hyperplastic lesions. COX-2 was up-regulated in 10 out of 11 adenomas. Interestingly, COX-2 was down-regulated in all examined adenocarcinomas. Further details are summarized in Table V, in which COX-2 expression levels are classified into four groups (–, ±, + and ++) by staining strength. Moreover, VEGF immunostaining revealed that VEGF was observed in hyperplasia (6/8) and adenomas (8/11) but not in adenocarcinomas (Figures 4D-F).

COX-2 expression was also observed in macrophage and non-ciliated bronchiolar epithelial cells (clara cells) of human normal lung tissue, epithelial cells of atypical adenomatous hyperplasia and tumor cells of human lung tumors (Noguchi type B).

Table V. *Immunohistochemical analysis of COX-2 expression in lung SOLs without indomethacin treatment.*

| Intensity | COX-2 | | |
|---|---|---|---|
| | Hyperplasias | Adenomas | Adenocarcinomas |
| – | 0/8 (0) | 1/11 (9) | 4/10 (40) |
| ± | 0/8 (0) | 3/11 (27) | 1/10 (10) |
| + | 5/8 (63) | 5/11 (45) | 0/10 (0) |
| ++ | 3/8 (38) | 2/11 (18) | 0/10 (0) |

–: Negative staining; ±: mixture lesion of – and +; +: positive staining; ++: strong-positive staining. Numbers in parentheses are percentages of mice with lung nodules.

## Discussion

In the present study, micro-CT with a respiratory gating system was shown to be a useful non-invasive tool for evaluating the effects of indomethacin on urethane-induced lung SOL development in mice. This study provides evidence that indomethacin is able to suppress lung tumorigenesis at multiple stages, especially the adenoma-to-adenocarcinoma stage (Table II). Moreover, indomethacin treatment effectively suppressed the size of urethane-induced lung tumors (Table III).

In this urethane-induced lung tumor model, DNA mutations in lung epithelial cells are reported. Several tumor-susceptibility genes, such as cell-cycle-related genes (*Brca1*, *Cdkn2a/b*) and cell growth and angiogenesis-related genes (*Fos, Jun, Kras, Pkcn* and *Tnfa*) are mutated (15-20). Indomethacin has been reported to inhibit only the activity of β-catenin and COX, but not of cyclin-dependent kinase, activator protein 1 (AP-1) (Fos/Jun) and nuclear factor-kappa B (NF-κB) (21, 22). Thus, one can speculate that indomethacin inhibits lung tumor growth (Table IV) through direct inhibition of COX-1 and COX-2, which might be induced by *Fos*, *Jun*, *Kras*, *Pkcn* and *Tnfa* mutation.

Prostaglandin $E_2$ is reported to induce VEGF and increase the angiogenic response (23, 24). Moreover, indomethacin is reported to inhibit blood vessel formation in tumor-induced *in vivo* angiogenesis assays using C3H/HeJ mice (25). As shown in this study, expression of COX-2 was confirmed in hyperplasia and adenoma in the mice by immunohistochemical assay (Figure 4 and Table V). Expression of COX-2 was also confirmed in the early-stage of human lung tumors (Figure 5). Interestingly, COX-2 was down-regulated in adenocarcinoma, which might be the result of gene instability, as observed in the progressive stage of lung cancer (7). These data suggest that COX-2 inhibitor may be useful in preventing human lung tumor development. Furthermore, VEGF expression in adenoma may be related to the progression of adenoma to adenocarcinoma (Figure 4), and indomethacin may inhibit this angiogenic response.

Our data also propose candidate factors related to malignant transformation, including well-known factors. Proposed factors could be tumor size, tumor growth speed,

characteristics of nodules on CT image, and an allowed time span for tumor growth. Table III demonstrates the possibility that tumor size could correlate with histopathological type, but correlation seems weak. Tumor growth speed could be a strong candidate. However, our present and previous data showed that adenocarcinoma grew from slow to fast (Figure 2A), and we concluded that growth speed might be a susceptibility factor. Among the fast growing nodules, a smooth surface of the nodule (Figures 2B-E) is one of the characteristics of adenocarcinoma. The characteristics of lung adenocarcinoma in CT images need to be further investigated in detail. Finally, we concluded that the time span allowed for tumorigenesis is the most important factor for malignant transformation because our data (Figure 2B) demonstrate that all nodules which were finally diagnosed as adenocarcinoma at the end of the experiment existed at the early-stage of this experiment. These results indicate that the whole span of administration of indomethacin is not required to achieve similar chemopreventive effects of indomethacin, and experiments with several administration time spans are desired to obtain informative data.

In conclusion, our results provide evidence that respiratory-gated micro-CT scanning of live mice has the potential to evaluate the effects of cancer chemopreventive agents on lung tumorigenesis. Using this method, indomethacin revealed chemopreventive effects on lung tumorigenesis. Thus, this novel approach could be used as a screening technique for chemopreventive agents using a reduced number of sacrificed animals compared to other methods. Moreover, this novel approach may also have an impact on the study of natural lung tumor regression and of cancer therapeutic agents.

## Acknowledgements

This work was supported by Grants-in-Aid for Cancer Research, for the Third-Term Comprehensive 10-Year Strategy for Cancer Control from the Ministry of Health, Labour and Welfare of Japan.

## References

1 Jemal A, Murray T, Ward E, Samuels A, Tiwari RC, Ghafoor A, Feuer EJ and Thun MJ: Cancer statistics 2005. CA Cancer J Clin *55*: 10-30, 2005.

2 Thun MJ, Namboodiri MM and Heath CW Jr.: Aspirin use and reduced risk of fatal colon cancer. N Engl J Med *325*: 1593-1596, 1991.

3 Akasu T, Yokoyama T, Sugihara K, Fujita S, Moriya Y and Kakizoe T: Peroral sustained-release indomethacin treatment for rectal adenomas in familial adenomatous polyposis: A pilot study. Hepatogastroenterology *49*: 1259-1261, 2002.

4 Sandler RS, Halabi S, Baron JA, Budinger S, Paskett E, Keresztes R, Petrelli N, Pipas JM, Karp DD, Loprinzi CL, Steinbach G and Schilsky R: A randomized trial of aspirin to prevent colorectal adenomas in patients with previous colorectal cancer. N Engl J Med *348*: 883-890, 2003.

5 Baron JA, Cole BF, Sandler RS, Haile RW, Ahnen D, Bresalier R, McKeown-Eyssen G, Summers RW, Rothstein R, Burke CA, Snover DC, Church TR, Allen JI, Beach M, Beck GJ, Bond JH, Byers T, Greenberg ER, Mandel JS, Marcon N, Mott LA, Pearson L, Saibil F and van Stolk RU: A randomized trial of aspirin to prevent colorectal adenomas. N Engl J Med *348*: 891-899, 2003.

6 Reddy BS: Studies with the azoxymethane-rat preclinical model for assessing colon tumor development and chemoprevention. Environ Mol Mutagen *44*: 26-35, 2004.

7 Bauer AK, Malkinson AM and Kleeberger SR: Susceptibility to neoplastic and non-neoplastic pulmonary diseases in mice: genetic similarities. Am J Physiol Lung Cell Mol Physiol *287*: L685-703, 2004.

8 Moysich KB, Menezes RJ, Ronsani A, Swede H, Reid ME, Cummings KM, Falkner KL, Loewen GM and Bepler G: Regular aspirin use and lung cancer risk. BMC Cancer *2*: 31, 2002.

9 Moody TW, Leyton J, Zakowicz H, Hida T, Kang Y, Jakowlew S, You L, Ozbun L, Zia H, Youngberg J and Malkinson A: Indomethacin reduces lung adenoma number in A/J mice. Anticancer Res *21*: 1749-1755, 2001.

10 Vane JR, Bakhle YS and Botting RM: Cyclooxygenases 1 and 2. Annu Rev Pharmacol Toxicol *38*: 97-120, 1998.

11 Hori Y, Takasuka N, Mutoh M, Kitahashi T, Kojima S, Imaida K, Suzuki M, Kohara K, Yamamoto S, Moriyama N, Sugimura T and Wakabayashi K: Periodic analysis of urethane-induced pulmonary tumors in living A/J mice by respiration-gated X-ray microcomputed tomography. Cancer Sci *99*: 1774-1777, 2008.

12 Niho N, Mutoh M, Komiya M, Ohta T, Sugimura T and Wakabayashi K: Improvement of hyperlipidemia by indomethacin in Min mice. Int J Cancer *121*: 1665-1669, 2007.

13 Ulrich M: International Classification of Rodent Tumors: Mouse. New York: Springer-Verlag, 2001.

14 Noguchi M, Morikawa A, Kawasaki M, Matsuno Y, Hirohashi S, Kondo H and Shimosato Y: Small adenocarcinoma of the lung. Histologic characteristics and prognosis. Cancer *75*: 2844-2852, 1995.

15 Festing MF, Lin L, Devereux TR, Gao F, Yang A, Anna CH, White CM, Malkinson AM and You M: At least four loci and gender are associated with susceptibility to the chemical induction of lung adenomas in A/J x BALB/c mice. Genomics *53*: 129-136, 1998.

16 Gariboldi M, Manenti G, Canzian F, Falvella FS, Radice MT, Pierotti MA, Della Porta G, Binelli G and Dragani TA: A major susceptibility locus to murine lung carcinogenesis maps on chromosome 6. Nat Genet *3*: 132-136, 1993.

17 Manenti G, Gariboldi M, Elango R, Fiorino A, De Gregorio L, Falvella FS, Hunter K, Housman D, Pierotti MA and Dragani TA: Genetic mapping of a pulmonary adenoma resistance (*Par1*) in mouse. Nat Genet *12*: 455-457, 1996.

18 Pataer A, Nishimura M, Kamoto T, Ichioka K, Sato M and Hiai H: Genetic resistance to urethan-induced pulmonary adenomas in SMXA recombinant inbred mouse strains. Cancer Res *57*: 2904-2908, 1997.

19 Lin L, Festing MF, Devereux TR, Crist KA, Christiansen SC, Wang Y, Yang A, Svenson K, Paigen B, Malkinson AM and You M: Additional evidence that the *K-ras* protooncogene is a candidate for the major mouse pulmonary adenoma susceptibility (*Pas-1*) gene. Exp Lung Res *24*: 481-497, 1998.

20 Miyashita N and Moriwaki K: H-2-controlled genetic susceptibility to pulmonary adenomas induced by urethane and 4-nitroquinoline 1-oxide in A/Wy congenic strains. Jpn J Cancer Res *78*: 494-498, 1987.

21 Dihlmann S, Klein S and Doeberitz Mv MK: Reduction of beta-catenin/T-cell transcription factor signaling by aspirin and indomethacin is caused by an increased stabilization of phosphorylated beta-catenin. Mol Cancer Ther *2*: 509-516, 2003.

22 Tegeder I, Pfeilschifter J and Geisslinger G: Cyclooxygenase-independent actions of cyclooxygenase inhibitors. FASEB J *15*: 2057-2072, 2001.

23 Pai R, Szabo IL, Soreghan BA, Atay S, Kawanaka H and Tarnawski AS: PGE2 stimulates VEGF expression in endothelial cells *via* ERK2/JNK1 signaling pathways. Biochem Biophys Res Commun *286*: 923-928, 2001.

24 Uefuji K, Ichikura T and Mochizuki H: Cyclooxygenase-2 expression is related to prostaglandin biosynthesis and angiogenesis in human gastric cancer. Clin Cancer Res *6*: 135-138, 2000.

25 Rozic JG, Chakraborty C and Lala PK: Cyclooxygenase inhibitors retard murine mammary tumor progression by reducing tumor cell migration, invasiveness and angiogenesis. Int J Cancer *93*: 497-506, 2001.

*Received August 13, 2012*
*Revised October 4, 2012*
*Accepted October 5, 2012*

RESEARCH ARTICLE

# Suppressive Effect of Pioglitazone, a PPAR Gamma Ligand, on Azoxymethane-induced Colon Aberrant Crypt Foci in KK-$A^y$ Mice

**Toshiya Ueno[1,3], Naoya Teraoka[1], Shinji Takasu[1], Katsuya Nakano[1,3], Mami Takahashi[2], Masafumi Yamamoto[2], Gen Fujii[1], Masami Komiya[1], Akinori Yanaka[3], Keiji Wakabayashi[4], Michihiro Mutoh[1]**

## Abstract

**Obesity is an established risk factor for colorectal cancer. Pioglitazone is a peroxisome proliferator-activated receptorγ (PPARγ) agonist that induces differentiation in adipocytes and induces growth arrest and/or apoptosis *in vitro* in several cancer cell lines. In the present study, we investigated the effect of pioglitazone on the development of azoxymethane-induced colon aberrant crypt foci (ACF) in KK-$A^y$ obesity and diabetes model mice, and tried to clarify mechanisms by which the PPARγ ligand inhibits ACF development. Administration of 800 ppm pioglitazone reduced the number of colon ACF / mouse to 30% of those in untreated mice and improved hypertrophic changes of adipocytes in KK-$A^y$ mice with significant reduction of serum triglyceride and insulin levels. Moreover, mRNA levels of adipocytokines, such as leptin, monocyte chemoattractant protein-1 and plasminogen activator inhibitor-1, in the visceral fat were decreased. PCNA immunohistochemistry revealed that pioglitazone treatment suppressed cell proliferation in the colorectal epithelium with elevation of p27 and p53 gene expression. These results suggest that pioglitazone prevented obesity-associated colon carcinogenesis through improvement of dysregulated adipocytokine levels and high serum levels of triglyceride and insulin, and increase of p27 and p53 mRNA levels in the colorectal mucosa. These data indicate that pioglitazone warrants attention as a potential chemopreventive agent against obesity-associated colorectal cancer.**

**Key words:** Pioglitazone - obesity - PPAR gamma - aberrant crypt foci

*Asian Pacific J Cancer Prev,* **13**, 4067-4073

## Introduction

Colorectal cancer is one of the common cancers in developed countries including Japan. Many epidemiological studies have suggested colorectal cancer correlates with obesity, a high-fat diet and hyperlipidemia, especially, hypertriglyceridemia and high levels of low-density lipoprotein cholesterol (Le Marchand et al., 1997; Bruce et al., 2000). Assumed mechanisms underlying obesity-associated cancer development could involve insulin resistance, chronic inflammation and dyslipidemia caused by dysregulation of adipocytokine production. Among adipocytokines, increased levels of leptin, plasminogen activator inhibitor-1 (PAI-1), and decreased levels of adiponectin are demonstrated to play an important role in colorectal carcinogenesis (van Kruijsdijk et al., 2009).

Recently, we have reported that KK-$A^y$ mice, carrying the Agouti yellow gene ($A^y$) and resultant hyperphagia (Nakamura et al., 1967), are highly susceptible to azoxymethane (AOM)-induced colorectal carcinogenesis (Teraoka et al., 2011). The KK-$A^y$ mice exhibited severe abdominal obesity, hypertriglyceridemia and hyperinsulinemia. Moreover, serum pro-inflammatory adipocytokines such as interleukin-6 (IL-6), leptin and Pai-1 in KK-$A^y$ mice were elevated and adiponectin was decreased compared to those in lean C57BL/6J mice. Among them, serum leptin levels were the highest in KK-$A^y$ mice. Those features of KK-Ay mice could explain their high susceptibility to AOM-induced colorectal carcinogenesis, and suggests they could be useful to evaluate chemopreventive agents against obesity-associated colorectal cancer.

Peroxisome proliferator-activated receptorγ (PPARγ) is a key nuclear hormone receptor of lipid metabolisms and regulates several gene transcriptions associated with

*[1]Division of Cancer Prevention Research, [2]Central Animal Division, National Cancer Center Research Institute, Tokyo, [3]Faculty of Pharmaceutical Sciences, Tokyo University of Science, Chiba, [4]Graduate School of Integrated Pharmaceutical and Nutritional Sciences, University of Shizuoka, Shizuoka , Japan *For correspondence: mimutoh@ncc.go.jp*

differentiation, growth arrest and apoptosis (Fisher et al., 1998; Sporn et al., 2000). PPARγ directly activates lipoprotein lipase (LPL) promoter activity, and induces LPL, which catabolizes triglycerides to monoglycerides (Schoonjans et al., 1996). Activation of PPARγ also induces terminal differentiation of adipocytes linking to downsizing of hypertrophic adipotissue. Meanwhile, PPARγ induces growth arrest and apoptosis in several cancer cell lines, including colon, esophageal squamous, gastric and pancreatic cancer cells (Takahashi et al., 1999; Shimada et al., 2002; Rumi et al., 2002; Itami et al., 2001). Pioglitazone is a selective PPARγ agonist that improves hyperlipidemia and hyperglycemia in obese diabetic animals and humans (Sohda et al., 1990; Ikeda et al., 1990; Sakamoto et al., 2000). Although side effects, such as weight gain, peripheral edema, precipitation of chronic heart failure and an increase in bone fractures limit widespread use of pioglitazone, pioglitazone is a useful antidiabetic drug, which is well tolerated in the majority of patients (Shah et al., 2010). Previously, we have reported that pioglitazone induced LPL and suppressed concurrently both hyperlipidemia and intestinal polyp formation in *Apc*-deficient Min mice, a model mouse for familial adenomatous polyposis (Niho et al., 2003). Thus, pioglitazone may be a potential chemopreventive agent against colorectal carcinogenesis. Furthermore, pioglitazone may be a more useful chemopreventive agent against obesity-associated cancers, such as mammary cancer (Bojková et al., 2010).

In the present study, we investigated the effects of pioglitazone on the development of AOM-induced aberrant crypt foci (ACF) in obese KK-$A^y$ mice. The novelty of this study is investigating the effect of pioglitazone in obese mice with retention of leptin and leptin receptor genes, in which we are able to examine actions of several molecules, such as adipocytokine, triglyceride and insulin with intact leptin signaling. The results demonstrated that pioglitazone prevented obesity-associated colorectal carcinogenesis through improving dysregulated levels of adipocytokines, especially leptin, insulin and lipids. Furthermore, another mechanism underlying the suppressive effect of pioglitazone is discussed with reference to induction of cell cycle-related genes.

## Materials and Methods

*Animals and chemicals*

Female 5-week-old KK-$A^y$/TaJcl (KK-$A^y$) and C57BL/6J mice were purchased from CLEA Japan (Tokyo, Japan), and acclimated to laboratory conditions for 1 week. Five mice were housed per plastic cage with sterilized softwood chips as bedding in a barrier-sustained animal room at 24 ± 2°C and 55% humidity on a 12 hr light/dark cycle and fed AIN-76A powdered basal diet (CLEA Japan) and water. The animals in each cage were all in the same treatment group. The pioglitazone, {(±)-5-[4-[2-(5-ethyl-2-pyridyl)ethoxy] benzyl]thiazolidine-2,4-dione monohydrochloride}, was kindly provided by Takeda Chemical Industries, Ltd. (Osaka, Japan).

*Experimental protocol for KK-$A^y$ mice treated with azoxymethane and pioglitazone*

For the induction of ACF by AOM (Nard Institute, Ltd., Amagasaki, Japan), 6-week-old female KK-$A^y$ (n=10) were given intraperitoneal injections of AOM (200 μg/mouse) in 0.9% NaCl saline once a week for 3 weeks. Five mice were also injected with saline as a control group. At the same time of first intraperitoneal injections, pioglitazone was administrated at concentrations of 400 or 800 ppm in basal diet. The dosage of pioglitazone was determined by our previous experiment (Niho et al., 2003). Food and water were available ad libitum. The animals were observed daily for clinical signs and mortality. Body weights and food and water consumption were measured weekly. All the mice were anesthetized with ether and sacrificed at the age of 13 weeks, the organs, including intestinal tract, heart, kidneys, liver, lungs, spleen and visceral fat, were excised and were also observed macroscopically and blood samples from the caudal vena cava were collected. A part of visceral adipose tissue and liver tissue of KK-$A^y$ mice with and without AOM treatment, and colon mucosa of KK-$A^y$ mice without AOM treatment were rapidly deep-frozen in liquid nitrogen and stored at -80°C for further experiments. The experiments were performed according to the "Guidelines for Animal Experiments in the National Cancer Center" and were approved by the Institutional Ethics Review Committee for Animal Experimentation in the National Cancer Center.

*Assessment of AOM-induced colorectal ACF*

The intestinal tract was removed, the colorectum opened longitudinally and fixed flat between sheets of filter paper in 10% buffered formalin. After dividing the colorectum into the proximal segment and rectum (1.5 cm in length), halves of the remainder were divided into the middle and distal segment. These were stained with 0.2% methylene blue (Merck, Darmstadt, Germany) and the mucosal surface was assessed for ACF with a stereoscopic microscope, as previously reported (Bird et al., 1987).

*Analysis of visceral adiposity*

The images of visceral and subcutaneous fat were obtained by a cone-beam micro-CT scanner (eXplore Locus, General Electric Healthcare, Ontario, Canada) scanning from the first lumbar vertebra to the pubic bone. The volumes of the fat were analyzed by MicroView software (General Electric Healthcare).

*Real-time polymerase chain reaction analysis*

Total RNA was isolated from tissues by using Isogen (Nippon Gene, Tokyo, Japan), and treated with DNase I (Invitrogen, Carlsbad, CA, USA). One-μg RNA in a

**Table 1. Development of Colorectal ACF in KK-$A^y$ Mice Treated with AOM and Pioglitazone**

| Pioglitazone (ppm) | No. of mice with ACF | No. of ACF / colorectum | | | | | Mean no. of ACs / focus |
|---|---|---|---|---|---|---|---|
| | | Proximal | Middle | Distal | Rectum | Total | |
| 0 | 11 / 11 | 5.9 ± 3.3 | 19.1 ± 8.2 | 18.6 ± 5.2 | 6.9 ± 1.9 | 50.5 ± 13.9 | 1.6 ± 0.2 |
| 400 | 10 / 10 | 1.6 ± 2.6 ** | 6.5 ± 3.6 ** | 22.2 ± 9.3 | 9.7 ± 5.7 | 40.0 ± 13.4 | 1.4 ± 0.2 |
| 800 | 10 / 10 | 0.1 ± 0.3 ** | 3.8 ± 2.3 ** | 19.6 ± 6.2 | 8.4 ± 2.8 | 31.9 ± 6.6 * | 1.5 ± 0.2 |

Data are means ± SD. *p<0.05, **p<0.01 vs 0 ppm

final volume of 20 μL was used for synthesis of cDNA using an Omniscript® RT Kit (Qiagen, Hilden, Germany) with an oligo (dT) primer. Real-time PCR was carried out using a DNA Engine OpticonTM 2 (MJ Japan Ltd., Tokyo, Japan) with SYBR Green Real-time PCR Master Mix (Toyobo Co., Osaka, Japan). Primers for mouse adiponectin (5'-AGGATGCTACTGTTGCAAGCTCTC, 3'- CAGTCAGTTGGTATCATGGTAGAG), GAPDH (5'- TTGTCTCCTGCGACTTCA, 3'- CACCACCCTGTTGCTGTA), IL-6 (5'- ACAACCACGGCCTTCCCTACTT, 3'- CACGATTTCCCAGAGAACATGTG), leptin (5'- CCAAAACCCTCATCAAGACC, 3'- GTCCAACTGTTGAAGAATGTCCC), LPL (5'- GGATCCGTGGCCGCAGCAGACGCAGGA, 3'- GAATTCCATCCAGTTGATGAATCTGGCCAC), monocyte chemoattractant protein (MCP-1) (5'- CCACTCACCTGCTGCTACTCAT, 3'- TGGTGATCCTCTTGTAGCTCTCC), Ob-Rbl (5' Primer- CCATCTTTTATATGATCTGCCTGAAGT, 3' Primer- TGCATTGGACAGTCTGAAAGCT), Pai-1 (5'- ACAGCCTTTGTCATCTCAGCC, 3'- AGGGTTGCACTAAACATGTCAG), tumor necrosis factor-a(TNF-a) (5'- TGTGCTCAGAGCTTTCAACAAC, 3'- GCCCATTTGAGTCCTTGATG), p27 (5'- TCTCAGGCAAACTCTGAGGA, 3'- CTTCCTCATCCCTGGACACT), p53 (5'- CCCCAGGATGTTGAGGAGTTT, 3'- TTGAGAAGGGACAAAAGATGACA) were employed (Teraoka et al., 2011; Niho et al., 2005; Turmelle et al., 2006; Xiao et al., 2009). To assess the specificity of each primer set, amplicons generated from the PCR reaction were analyzed for melting curves.

*Measurement for serum lipids, adipocytokine and insulin*

Serum levels of triglycerides and total cholesterol were measured as reported (Niho et al., 2003). Serum levels of adiponectin, interleukin-1β (IL-1β), IL-6, MCP-1, leptin and insulin were measured using mouse adiponectin immunoassay (R&D systems, Inc., Minneapolis, MN, USA), mouse procarta® cytokine assay (Affymetrix, Inc., Santa Clara, CA, USA), a mouse leptin enzyme-linked immunosorbent assay kit (B-Bridge International, Inc., Cupertino, CA, USA) and a mouse insulin kit (Millipore Corp., Billerica, MA, USA).

*Immunohistochemical analysis*

The colon (segment of middle and distal) after analysis of colon ACF formation and the liver and the visceral fat were sliced and processed to sections stained with hematoxylin and eosin (H&E). Sections of middle and distal colon were also stained immunohistochemically with antibodies against proliferation cell nuclear antigen (PCNA; DAKO, Carpinteria, CA, USA) used at 200 x dilution. The number of PCNA positive cells was measured in a crypt from three different arbitrarily selected points in colon mucosa (n=5). The extent of enlargement of adipocytes was evaluated by quantification of the number of adipocyte nuclei observed in the field (x 200) of fat tissue in KK-$A^y$ mice.

*Statistical analysis*

The significance of difference in the number of AOM-induced colorectal ACF, serum lipid levels and serum cytokine levels was analyzed using Dunnett's multiple comparison test and other statistical analyses were performed with Student's t-test. Differences were considered to be statistically significant at $p<0.05$.

## Results

*Suppression of the numbers of AOM-induced colorectal ACF in KK-Ay mice by pioglitazone*

To determine the effect of pioglitazone on colorectal ACF development in obese KK-$A^y$ mice, KK-$A^y$ mice were treated with AOM and pioglitazone. Administration of pioglitazone did not significantly effect food intake, behavior or body weight changes during the experiment periods. Final body weights in 13-week-old female KK-$A^y$ mice untreated, treated with 400 ppm pioglitazone and 800 ppm pioglitazone were 45.7 ± 3.1 (mean ± SD), 40.0 ± 3.4 and 42.0 ± 3.5 g, respectively.

Table 1 shows data for the numbers and distribution of colorectal ACF in KK-$A^y$ mice with or without pioglitazone. All KK-Ay mice treated with AOM developed ACF in the colorectum at 13 weeks. The total numbers of ACF in the groups treated with pioglitazone at 400 and 800 ppm doses were reduced to 79 and 63% ($p<0.05$) of the control value, respectively. Of note, the number of ACF in the proximal and middle parts of the colon in the mice fed diet containing 400 and 800 ppm pioglitazone were reduced significantly ($p<0.01$). There were no significant differences in the mean numbers of ACs per focus among each group.

*Improvement of fatty change in the liver and hypertrophy of adipocytes in the visceral fat tissue by pioglitazone*

To clarify the effects of AOM and pioglitazone on other tissue, histopathological examination were

**Table 2. Amount of Fat Tissue in KK-*Ay* Mice Treated with AOM and Pioglitazone**

| Pioglitazone (ppm) | Visceral fat (g) | Subcutaneous fat (g) | Total (g) |
|---|---|---|---|
| 0 | 6.2 ± 0.9 | 2.0 ± 0.4 | 8.2 ± 1.2 |
| 800 | 4.2 ± 0.4 ** | 1.6 ± 0.1 * | 5.9 ± 0.5 ** |

Data are means ± SD. *p<0.05, **p<0.01 vs 0 ppm; Amount of fat tissue was analyzed by micro-CT

**Table 3. Levels of Serum Lipids and Insulin in KK-*Ay* Mice Treated with AOM and Pioglitazone**

| Pioglitazone (ppm) | Triglycerides (mg / dL) | Total cholesterol (mg / dL) | Insulin (ng / mL) |
|---|---|---|---|
| 0 | 502.0 ± 128.4 | 103.8 ± 19.3 | 39.5 ± 2.8 |
| 400 | 262.8 ± 81.2** | 89.7 ± 10.9 | 3.5 ± 1.6** |
| 800 | 254.3 ± 62.3 ** | 97.7 ± 16.8 | 4.4 ± 3.5 ** |

Data are means ± SD. **p<0.01 vs 0 ppm

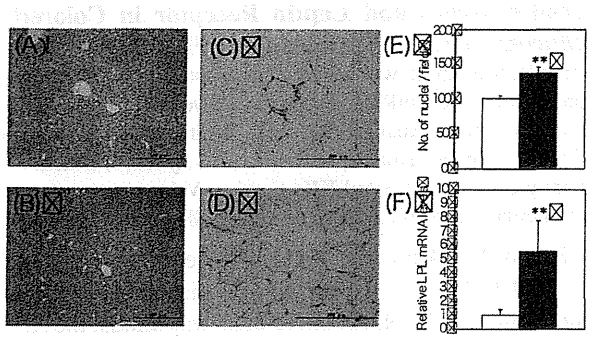


**Figure 1. Fatty Change in the Liver and Size of Adipocytes in the Visceral Fat Tissue.** (A, B) Representative histopathological sections (H&E) of the liver in KK-*Ay* mice and the liver of the mice treated with 800 ppm pioglitazone are shown, respectively. (C, D) Representative histopathological sections (H&E) of the visceral fat in KK-*Ay* mice and the mice treated with 800 ppm pioglitazone, respectively. (E) Numbers of nuclei of visceral fat cells in a microscopical field were counted and are shown. (F) Hepatic LPL mRNA expression levels were examined by real-time PCR analysis. GAPDH mRNA was used to normalize the data. Values were set at 1.0 in untreated control Data are means ± SE (n=5). **, p<0.01.

performed on the liver and visceral fat tissue. The weights of liver at the end of experiments in KK-*Ay* mice treated with AOM and 0, 400 and 800 ppm pioglitazone treated group were 1.7 ± 0.1 (mean ± SD), 1.7 ± 0.2 and 1.9 ± 0.2 g, respectively. As shown in Figure 1A, fatty change of the liver was observed in KK-*Ay* mice by histopathological examination, and was clearly improved by administration of 800 ppm pioglitazone (Figure 1B).

The volume of visceral and subcutaneous fat was measured by a micro-CT, and these amounts are summarized in Table 2. Treatment with 800 ppm pioglitazone in KK-*Ay* mice significantly decreased the amount of visceral fat (p<0.01), subcutaneous fat (p<0.05) and total fat (p<0.01) compared with those of the untreated control. The amounts of mesenteric fat tissue in KK-*Ay* mice untreated, treated with 400 ppm and 800 ppm pioglitazone were 1.5 ± 0.4 (mean ± SD), 0.7 ± 0.2 (p<0.01 vs 0 ppm) and 0.7 ± 0.3 g (p<0.01 vs 0 ppm), respectively. Histopathological examination of visceral adipose tissue clearly showed that the size of adipocytes in visceral adipose tissue in KK-*Ay* mice treated with 800 ppm pioglitazone was smaller than that in untreated control mice (Figure 1C and 1D). Moreover, the number of adipocyte nuclei observed in one field of visceral fat tissue under the microscope (x200) in KK-*Ay* mice was 101.0 ± 10.0, and treatment with 800 ppm pioglitazone significantly increased the number to 137.0 ± 20.0 (p<0.01) (Figure 1E).

*Improvement of the levels of lipids, insulin and adipocytokines in serum of KK-Ay mice treated with pioglitazone*

To evaluate the effects of pioglitazone on the size reduction of adipocytes in the visceral fat tissue, the levels of serum lipids, insulin and adipocytokines were measured, and are summarized in Tables 3 and 4. The average serum levels of triglycerides and insulin, but not total cholesterol of KK-*Ay* mice treated with AOM and 400 ppm or 800 ppm pioglitazone were significantly decreased compared with those of KK-*Ay* mice treated AOM alone (Table 3). Thus, we investigated the effects of pioglitazone on hepatic mRNA levels of LPL,

**Table 4. Levels of Serum Adipocytokines in KK-*Ay* Mice Treated with AOM and Pioglitazone**

| Pioglitazone (ppm) | Adiponectin (mg / mL) | IL-1b (pg / mL) | IL-6 (pg / mL) | MCP-1 (pg / mL) | Leptin (ng / mL) |
|---|---|---|---|---|---|
| 0 | 12.7 ± 1.5 | 54.1 ± 17.6 | 26.4 ± 20.4 | 155.1 ± 37.2 | 140 ± 31.7 |
| 400 | 14.5 ± 0.9 | 36.6 ± 6.80* | 12.2 ± 2.60 | 138.6 ± 26.9 | 45.9 ± 27.2** |
| 800 | 27.9 ± 2.0 ** | 51.4 ± 10.7 | 35.0 ± 20.8 | 99.3 ± 36.1** | 46.5 ± 21.7** |

Data are means ± SD. **p<0.01 vs 0 ppm, . *p<0.05 vs 0 ppm

**Table 5. PCNA Immunostaining in Middle or Distal Colon of KK-*Ay* Mice Treated with AOM and 800 ppm Pioglitazone**

| Pioglitazone (ppm) | Cells / crypt | | PCNA positive cell / crypt | | % of PCNA positive cells / total cells crypt | |
|---|---|---|---|---|---|---|
| | Middle | Distal | Middle | Distal | Middle | Distal |
| 0 | 42.0 ± 4.2 | 39.6 ± 3.3 | 17.0 ± 4.7 | 12.2 ± 2.7 | 41.2 ± 11.4 | 30.6 ± 7.0 |
| 800 | 38.6 ± 3.5 | 34.2 ± 3.9 | 12.9 ± 2.7 | 12.1 ± 2.7 | 33.4 ± 5.8 | 35.8 ± 8.8 |

Data are means ± SD

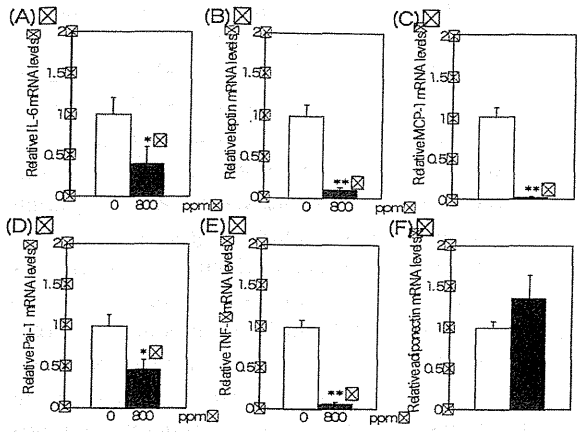


**Figure 2. Relative Expression Levels of Adipocytokine mRNA in Visceral Fat Tissue of KK-Ay Mice.** Real-time PCR analysis was performed to obtain IL-6 (A), leptin (B), MCP-1 (C), Pai-1 (D), TNF-α (E) and adiponectin (F) mRNA expression levels. GAPDH mRNA was used to normalize the data. White, untreated control group. Black, 800 ppm pioglitazone treated group. Values were set at 1.0 in the untreated control. Data are means ± SE (n=5). *, p<0.05, **, p<0.01.

which catabolizes triglycerides to monoglycerides. Administration of 800 ppm pioglitazone increased 5.6-fold the hepatic LPL mRNA levels compared with those of untreated control levels (Figure 1F). The serum adiponectin level was also significantly increased and serum levels of leptin and MCP-1 were significantly decreased in KK-Ay mice treated with 800 ppm pioglitazone compared with untreated KK-$A^y$ mice ($p<0.01$). Significant differences were also obtained in serum levels of IL-1β and leptin in KK-$A^y$ mice treated with 400 ppm pioglitazone (Table 4).

*Improvement of the levels of adipocytokines in visceral fat tissue of KK-Ay mice treated with pioglitazone*

Data for the mRNA expression levels of adipocytokines in visceral fat tissue are shown in Figure 2. The mRNA expression levels of IL-6, leptin, MCP-1, Pai-1 and TNF-α in KK-$A^y$ mice treated with AOM and 800 ppm pioglitazone were significantly decreased compared with those of KK-Ay mice treated with AOM alone. On the other hand, treatment of 800 ppm pioglitazone had a tendency to up-regulate the mRNA expression of adiponectin compared with untreated KK-$A^y$ mice.

*Validation of colon epithelial cell proliferation in KK-Ay mice treated with pioglitazone and/or AOM*

To investigate the effect of pioglitazone treatment on epithelial cell proliferation of colon mucosa in KK-$A^y$ mice, the amount of cells in S phase and expression of cell cycle-related gene (p27 and p53) were examined. PCNA immunohistochemical staining revealed that administration of 800 ppm pioglitazone had a tendency to suppress cell proliferation in the colon mucosa in KK-$A^y$ mice. As shown in Table 5, the total cells per crypt in middle colon mucosa of KK-$A^y$ mice and the mice treated with 800 ppm pioglitazone were 41.2 ± 11.4 and 33.4 ± 5.8, and PCNA positive cells in those mice were 17.0 ± 4.7 and 12.9 ± 2.7, respectively. In distal colon mucosa, the number of PCNA positive cells was almost the same between the each group. Related to cell proliferation, leptin elicits its biological activity through Ob-Rbl, and downstream targets, Akt, Erk and STAT3, may stimulate cell growth signaling with modifying cell cycle-related genes. Thus we examined cell cycle-related genes, p27 and p53. The treatment with 800 ppm pioglitazone up-regulated the mRNA levels of p27 ($p<0.05$) and p53 ($p<0.05$), and down-regulated leptin receptor Ob-Rbl ($p<0.05$) in the colorectal mucosa of KK-$A^y$ mice without AOM compared with that of untreated control mucosa (Figure 3).

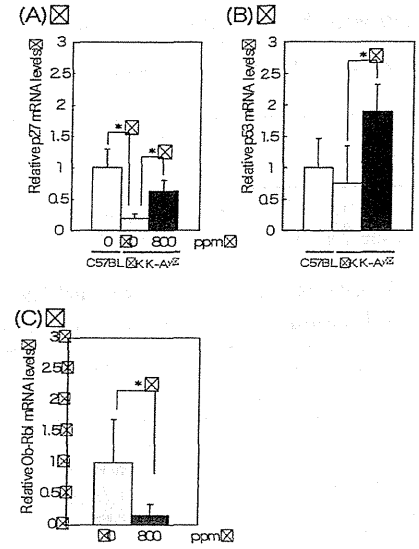


**Figure 3. Relative Expression Levels of Cell Cycle-related Genes and Leptin Receptor in Colorectal Mucosa of KK-*Ay* Mice and C57BL/6J Mice.** Real-time PCR analysis was performed to obtain p27 (A), p53 (B) and Ob-Rbl (C) mRNA expression levels. GAPDH mRNA was used to normalize the data. White, untreated control C57BL/6J mice. Dotted, untreated KK-*Ay* mice. Black, 800 ppm pioglitazone treated KK-*Ay* mice. Values were set at 1.0 in untreated control. Data are means ± SE (n=4). *, p<0.05.

## Discussion

In the present study, pioglitazone treatment decreased the number of AOM-induced ACF in obese KK-$A^y$ mice. This suppressive effect of pioglitazone might be explained by involvement of systemic improvement of dysregulated adipocytokine, triglyceride and insulin levels, and increase of mRNA levels of p27 and p53 in the colorectal mucosa of KK-$A^y$ mice. This study provided the evidence that pioglitazone could be a useful chemopreventive agent against obesity-associated colorectal cancer.

It has been reported that hypertrophic change of adipocytes evokes dysregulated adipocytokine production (Cowey et al., 2006; van Kruijsdijk et al., 2009). Thus, we examined the size of adipocytes in visceral adipose tissue in KK-$A^y$ mice treated with pioglitazone and found the

size to be much smaller than those in untreated control mice. These data are consistent with previous reports that PPARγ, a member of the nuclear receptor superfamily, stimulated preadipocyte differentiation, and reduced the size of adipocytes to the normal size (Schoonjans et al., 1996). Size reduction of adipocyte is suggested to improve insulin resistance along with reduced serum triglyceride levels. In fact, serum levels of triglycerides, insulin and leptin levels were decreased at a dose of 800 ppm pioglitazone, and serum adiponectin was increased. In addition, the expression of LPL was increased in the liver being related to reduction of serum triglyceride levels. It has been reported that the PPAR-responsible elements exist in the promoter region of the LPL gene, and indeed, pioglitazone increased hepatic expression levels of LPL. Moreover, the mRNA expression levels of IL-6, leptin, MCP-1, Pai-1 and TNF-α in visceral adipose were reduced by pioglitazone treatment, and adiponectin tended to be increased in the present study. It has been reported that PPARγ ligand inhibits Ob-Rbl mRNA expression in human hepatic stellate cells (Schoonjans et al., 1996). Several experiments using thiazolidinediones, selective ligands of PPARγ, revealed that PPARγ targets adiponectin, IL-6, MCP-1 and TNF-α and increase adiponectin expression levels but decrease the rest (Iwaki et al., 2003).

The expression of cell cycle-related genes (p27 and p53) in colorectal mucosa of KK-$A^y$ mice was down-regulated compared with those of C57BL/6J mice, which are generally used as non-obese, non-diabetic controls (Figure 3). P27 and p53, which belong to the Cip/Kip family of cyclin-dependent kinase inhibitors, play a key role in cell growth arrest (Polyak et al., 1994). The administration of 800 ppm pioglitazone increased the expression levels of low p27 and p53 mRNA levels observed in the colorectal mucosa of KK-$A^y$ mice. Leptin elicits its biological activity through Ob-Rbl, and downstream targets, Akt, Erk and STAT3, may stimulate cell growth signaling with modifying cell cycle-related genes. It has been reported that STAT3 would play both a positive regulatory role and a negative one for p27 expression (Fukada et al., 1998; Kortylewski et al., 1999). Thus, it is implicated that low p27 and p53 in the obese mice could be due to high serum levels of leptin in part, and that increased expression of p27 and p53 by pioglitazone treatment could due to a decrease of leptin expression. Of note, insulin and insulin-like growth factors are strong growth factors modifying cell cycle-related genes and may affect colorectal ACF development. The serum level of insulin, drastically decreased with pioglitazone, also could explain the effects of pioglitazone on ACF development. The ratio of contribution of the factors, such as adipocytokine, insulin and triglyceride should be revealed in the future.

It is interesting that pioglitazone suppressed AOM-induced ACF development in the upper portion of the colorectum (proximal and middle colon), but not lower portion (distal colon and rectum). To clarify the localized specific effect of pioglitazone, PCNA immunohistochemical staining was conducted in middle and distal colon. As a result, administration of 800 ppm pioglitazone had a tendency to reduce PCNA positive cells in the middle colon in KK-$A^y$ mice. Moreover, there were no significant differences in mRNA levels of p27 and p53 between the middle and distal parts (data not shown). Comparing the numbers of ACF in AOM-treated lean C57BL/6J mice with those of KK-$A^y$ mice, KK-$A^y$ mice increased the number of ACF in the proximal and middle colon (Teraoka et al., 2011). However, the effect of pioglitazone on different portions of the colon in obese mice could not be explained. Further examinations with novel aspects are needed to clarify the different action of pioglitazone on ACF development in the distal and middle colon.

In conclusion, pioglitazone has a potential benefit to suppress AOM-induced ACF development in obese KK-$A^y$ mice in a systematic and direct manner. Pioglitazone also could effectively suppress intestinal polyp development in Min mice (Niho et al., 2003). Thus, pioglitazone might be a good candidate for a chemopreventive agent against obesity-associated colorectal cancer. Meanwhile, a cohort study showed no clear associations between use of pioglitazone and reduced risk of colon cancer incidence in diabetes patients (Ferrara et al., 2011), with the limitation of short periods of follow up, less than 6 years, after the initiation of pioglitazone. Thus, further epidemiological studies with long periods of follow up are desired to evaluate pioglitazone, as a potential chemopreventative agent in humans.

## Acknowledgement

This work was supported by Grants-in-Aid for Cancer Research, for the Third-Term Comprehensive 10-Year Strategy for Cancer Control from the Ministry of Health, Labour, and Welfare of Japan, and also from the Yakult Bio-science Foundation. S.T. was the recipient of a Research Resident Fellowship from the Foundation for Promotion of Cancer Research.

## References

Bird RP (1987). Observation and quantification of aberrant crypts in the murine colon treated with a colon carcinogen: preliminary findings. *Cancer Letts*, **37**, 147-51.

Bojková B, Garajová M, Kajo K, et al (2010). Pioglitazone in chemically induced mammary carcinogenesis in rats. *Eur J Cancer Prev*, **19**, 379-84.

Bruce WR, Wolever TM, Giacca A (2000). Mechanisms linking diet and colorectal cancer: the possible role of insulin resistance. *Nutr Cancer*, **37**, 19-26.

Cowey S, Hardy RW (2006). The metabolic syndrome: A high-risk state for cancer? *Am J Pathol*, **169**, 1505-22.

Ferrara A, Lewis JD, Quesenberry CP Jr, et al (2011). Cohort study of pioglitazone and cancer incidence in patients with diabetes. *Diabetes Care*, **34**, 923-9.

Fisher B, Costantino JP, Wickerham DL, et al (1998). Tamoxifen for prevention of breast cancer: report of the national surgical adjuvant breast and bowel project P-1 study. *J Natl Cancer Inst*, **90**, 1371-88.

Fukada T, Ohtani T, Yoshida Y, et al (1998). STAT3 orchestrates contradictory signals in cytokine-induced G1 to S cell-cycle transition. *EMBO J*, **17**, 6670-7.

Ikeda H, Taketomi S, Sugiyama Y, et al (1990). Effects of pioglitazone on glucose and lipid metabolism in normal and insulin resistant animals. *Arzneimittelforschung*, **40**, 156–62.

Itami A, Watanabe G, Shimada-Itami A, et al (2001). Ligands for peroxisome proliferator-activated receptorγ inhibit growth of pancreatic cancers both in vitro and in vivo. *Int J Cancer*, **94**, 370–6.

Iwaki M, Matsuda M, Maeda N, et al (2003). Induction of adiponectin, a fat-derived antidiabetic and antiatherogenic factor, by nuclear receptors. *Diabetes*, **52**, 1655-63.

Kortylewski M, Heinrich PC, Mackiewicz A, et al (1999). Interleukin-6 and oncostatin M-induced growth inhibition of human A375 melanoma cells is STAT-dependent and involves upregulation of the cyclin-dependent kinase inhibitor p27/Kip1. *Oncogene*, **18**, 3742-53.

Le Marchand L, Wilkens LR, Kolonel LN, et al (1997). Association of sedentary lifestyle, obesity, smoking, alcohol use, and diabetes with the risk of colorectal cancer. *Cancer Res*, **57**, 4787-94.

Nakamura M, Yamada K (1967). Studies on a diabetic (KK) strain of the mouse. *Diabetologia*, **3**, 212-21.

Niho N, Mutoh M, Takahashi M, et al (2005). Concurrent suppression of hyperlipidemia and intestinal polyp formation by NO-1886, increasing lipoprotein lipase activity in Min mice. *Proc Natl Acad Sci USA*, **102**, 2970-4.

Niho N, Takahashi M, Shoji Y, et al (2003). Dose-dependent suppression of hyperlipidemia and intestinal polyp formation in Min mice by pioglitazone, a PPARγ ligand. *Cancer Sci*, **94**, 960-64.

Polyak K, Kato JY, Solomon MJ, et al (1994). p27Kip1, a cyclin-Cdk inhibitor, links transforming growth factor-beta and contact inhibition to cell cycle arrest. *Genes Dev*, **8**, 9-22.

Rumi MA, Sato H, Ishihara S, et al (2002). Growth inhibition of esophageal squamous carcinoma cells by peroxisome proliferator-activated receptor γ ligands. *J Lab Clin Med*, **140**, 17–26.

Sakamoto J, Kimura H, Moriyama S, et al (2000). Activation of human peroxisome proliferator-activated receptor (PPAR) subtypes by pioglitazone. *Biochem Biophys Res Commun*, **278**, 704–11.

Schoonjans K, Peinado-Onsurbe J, Lefebvre AM, et al (1996). PPARalpha and PPARgammma activators direct a distinct tissue-specific transcriptional response via a PPRE in the lipoprotein lipase gene. *EMBO J*, **15**, 5336-48.

Schoonjans K, Staels B, Auwerx J (1996). The peroxisome proliferator activated receptors (PPARs) and their effects on lipid metabolism and adipocyte differentiation. *Biochim Biophys Acta*, **1302**, 93-109.

Shah P, Mudaliar S (2010). Pioglitazone: side effect and safety profile. *Expert Opin Drug Saf*, **9**, 347-54.

Shimada T, Kojima K, Yoshiura K, et al (2002). Characteristics of the peroxisome proliferators activated receptor gamma (PPAR gamma) ligand induced apoptosis in colon cancer cells. *Gut*, **50**, 658-64.

Sohda T, Momose Y, Meguro K, et al (1990). Studies on antidiabetic agents. Synthesis of hypoglycemic activity of 5-[4-(pyridylalkoxy)benzyl]-2,4-thiazolidinediones. *Arzneimittelforschung*, **40**, 37–42.

Sporn MB, Suh N (2000). Chemoprevention of cancer. *Carcinogenesis*, **21**, 525-30.

Takahashi N, Okumura T, Motomura W, et al (1999). Activation of PPARγ inhibits cell growth and induces apoptosis in human gastric cancer cells. *FEBS Lett*, **455**, 135-9.

Teraoka N, Mutoh M, Takasu S, et al (2011). High susceptibility to azoxymethane-induced colorectal carcinogenesis in obese KK-Ay Mice. *Int J Cancer*, **102**, 79-87.

Turmelle YP, Shikapwashya O, Tu S, et al (2006). Rosiglitazone inhibits mouse liver regeneration. *FASEB J*, **20**, 2609-11.

van Kruijsdijk RC, van der Wall E, Visseren FL (2009). Obesity and cancer: the role of dysfunctional adipose tissue. *Cancer Epidemiol Biomarkers Prev*, **18**, 2569-78.

Xiao X, Wang Y, Gong H, et al (2009). Molecular evidence of senescence in corneal endothelial cells of senescence-accelerated mice. *Mol Vis*, **15**, 747-61.

# Novel Compound SK-1009 Suppresses Interleukin-6 Expression through Modulation of Activation of Nuclear Factor-KappaB Pathway

Misato Shimura,[a,d] Masafumi Yamamoto,[b] Gen Fujii,[a] Mami Takahashi,[b] Masami Komiya,[a] Nobuharu Noma,[a,d] Sei-ichi Tanuma,[d] Akinori Yanaka,[c,†] and Michihiro Mutoh*[,a]

[a] *Division of Cancer Prevention Research, National Cancer Center Research Institute;* [b] *Central Animal Division, National Cancer Center Research Institute; 5–1–1 Tsukiji, Chuo-ku, Tokyo 104–0045, Japan:* [c] *Faculty of Pharmaceutical Sciences, Tokyo University of Science; and* [d] *Division of Biochemistry, Faculty of Pharmaceutical Sciences, Tokyo University of Sciences; 2641 Yamazaki, Noda, Chiba 278–8510, Japan.*

Received June 29, 2012; accepted September 18, 2012; advance publication released online September 27, 2012

**Although interleukin-6 (IL-6) is an important biological mediator playing an indispensable role in inflammation and cancer, few inhibitors and suppressors are known. In the present study, the underlying mechanisms of a novel chemically synthesized compound SK-1009, which has suppressive properties on IL-6 production in human macrophage cells, were examined. SK-1009 suppressed IL-6 mRNA levels in human colon cancer cells. Thus, the influence of SK-1009 on transcription factor, nuclear factor-kappaB (NF-κB), which is involved in expression of the IL-6 gene was assessed. SK-1009 was found to suppress degradation of I-κB, an NF-κB inhibitory factor, and consequently inhibited the NF-κB activation pathway. The inhibitory property was almost the same as other NF-κB inhibitors, such as 5HPP-33. Thus, SK-1009 exerts a potent inhibitory effect on IL-6 expression, apparently mediated by modulation of activation of NF-κB transcription factor.**

**Key words** SK-1009; interleukin-6; nuclear factor-kappaB; colon

Interleukin 6 (interferon beta 2, IL-6) is a cytokine primarily produced at acute and chronic inflammation sites, and acts as both a pro-inflammatory and anti-inflammatory cytokine. IL-6 stimulates acute phase protein synthesis and neutrophil production in bone marrow. Moreover, it supports B cell growth and antagonizes regulatory T cells. IL-6 elicits its signals through a receptor complex of IL-6Rα and gp130. The function of the IL-6 gene is implicated in a wide variety of inflammation-associated diseases, such as diabetes mellitus, systemic juvenile rheumatoid arthritis and cancer.[1–3]

Patients with advanced and/or metastatic cancer have been reported to show high levels of IL-6 in their blood.[4–8] In animal models, *Apc*-deficient *Min* mice lacking the IL-6 gene decreased overall polyp numbers by 32% compared with IL-6 wild *Min* mice. The *Min* mouse has a mutation in the *Apc* tumor suppressor gene and develops intestinal polyps, and shows a 10-fold increase in serum IL-6 levels at 26 weeks of age.[9] On the other hand, pitavastatin is a novel chemically synthesized hydroxymethylglutaryl (HMG)-CoA reductase inhibitor, which was demonstrated to reduce intestinal polyp formation in *Min* mice. In the pitavastatin experiment, serum IL-6, leptin, and MCP-1 levels were decreased at a dose of 40 ppm.[10] Thus, IL-6 has been suggested to play an important role in colon/intestinal carcinogenesis.

Hence, there is an interest in developing anti-IL-6 agents for therapy against inflammation and cancer.[11,12] For instance, tocilizumab has been approved as a therapeutic agent for systemic juvenile rheumatoid arthritis. Indeed, it may be difficult to develop a small molecule, that selectively suppress IL-6 expression, but there are a very few small molecules reported to suppresses IL-6 expression. One of them is SK-1009 (Fig. 1). SK-1009 is a chemically synthesized compound, obtained from a screening of compound library. It has been reported to inhibit lipopolysaccharide (LPS)-induced IL-6 production in human macrophage cells, THP-1 (information from international patent WO2007/091313). However, underlying mechanisms of IL-6 suppression by SK-1009 are not elucidated in detail.

In the present study, we aimed to clarify the mechanisms by which SK-1009 suppresses IL-6 expression. We have investigated the effects of SK-1009 on IL-6 and tumor necrosis factorα (TNFα) expression levels in a human colon cancer cell line stimulated by TNFα. We found that SK-1009 effectively suppressed IL-6 expression through inhibition of activation of a transcription factor, nuclear factor-kappaB (NF-κB).

## MATERIALS AND METHODS

**Cells and Test Compounds** Human colon cancer cell lines, HCT116, RKO and SW480 cells (American Type Culture Collection, Manassas, VA, U.S.A.), were cultured in Dulbecco's modified Eagle's medium (DMEM) containing 5% fetal bovine serum (Hyclone Laboratories Inc., Logan, UT, U.S.A.) and antibiotics at 37°C in a humidified incubator

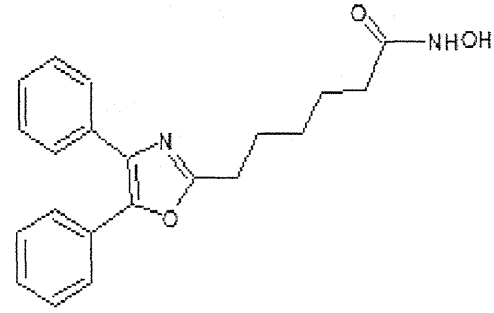


Fig. 1. Chemical Structure of SK-1009

The authors declare no conflict of interest.

†Present address: *Hitachi Medical Education and Research Center, Division of Clinical Medicine, Faculty of Medicine, University of Tsukuba; 2–1–1 Jonan-cho, Hitachi, Ibaraki 317–0077, Japan.*

*To whom correspondence should be addressed. e-mail: mimutoh@ncc.go.jp

with 5% $CO_2$. The IL-6 suppressor SK-1009, *N*-hydroxy-4,5-diphenyl-2-oxazolehexanamide, was chemically synthesized at Shizuoka Coffein Co., Ltd. Its structure is shown in Fig. 1. *In vitro* data showed that this compound reverse the inhibitory effects of LPS-induced IL-6 protein production in human macrophage cells, THP-1. $IC_{50}$ for SK-1009 is $2.7\times10^{-7}$ M, and was reported in international patent WO2007/091313. TNF$\alpha$ was purchased from PEPROTECH (Rock Hill, NJ, U.S.A.), NF-$\kappa$B inhibitors, 5HPP-33 and SM-7368 was purchased from Merck KGaA (Darmstadt, Germany). Catechin, dexamethasone and troglitazone were purchased from Sigma-Aldrich (St. Louis, MO, U.S.A.).

**Cell Viability Determined by 3-(4,5-Dimethylthiazol-2-yl)-2,5-diphenyltetrazolium Bromide (MTT) Assay** An hour before the end of treatment with TNF$\alpha$ and SK-1009, 0.5 mg/mL of MTT was added to the medium and incubated. The MTT formazan produced by living cells was dissolved with dimethyl sulfoxide and the absorbance at 590 nm was measured on a microplate reader.

**Real-Time Polymerase Chain Reaction (PCR) Analysis** Total RNA was isolated from cells using Isogen (Nippon Gene, Tokyo, Japan), treated with DNase (Invitrogen, Grand Island, NY, U.S.A.) and 3 $\mu$g aliquots in a final volume of 20 $\mu$L were used for synthesis of cDNA using an Omniscript RT Kit (Qiagen, Hilden, Germany) and randomized primer. Real-time PCR was carried out using a DNA Engine Opticon TM 2 (MJ Research, Waltham, MA, U.S.A.) with SYBR Green Realtime PCR Master Mix (Toyobo Co., Osaka, Japan) according to the manufacturer's instructions. Primers for IL-6 (5′-AAACAACCTGAACCTTCCAAAGA, 3′-GCAAGTCTCCTCATTGAATCCA), TNF$\alpha$ (5′-GAGGCCAAGCCCTGGTATG, 3′-CGGGCCGATTGATCTCAGC) and glyceraldehyde-3-phosphate dehydrogenase (GAPDH) (5′-TTGCCATCAATGACCCCTTCA, 3′-CGCCCCACTTGATTTTGGA) were employed. To assess the specificity of each primer set, amplicons generated from the PCR reaction were analyzed for melting curves and also by electrophoresis in 2% agarose gels.

**Luciferase Assay for NF-$\kappa$B Transcriptional Activity** To measure NF-$\kappa$B transcriptional activity, colon cancer cell lines HCT116, RKO and SW480 were seeded in 96-well plates ($2\times10^4$ cells/well). After 24 h incubation, cells were transiently transfected with 25 ng/well of pGL4.32 [*luc2P*/NF-$\kappa$kB RE/Hygro] (Promega Co., Madison, WI, U.S.A.) reporter plasmid and pGL4.73 [*hRluc*/SV40] (Promega) control plasmid using FuGENE® 6 Transfection Reagent (Roche Inc., Basel, Switzerland) according to the instructions provided by the manufacturer, and cultured for 24 h. The cells were then treated with test agents, and finally Firefly luciferase and Renilla luciferase activities were determined by Luciferase Assay Systems and Renilla Luciferase Assay Systems (Promega), respectively. Basal luciferase activity of untreated cells was set as 1.0. The percent luciferase activity with each treatment was calculated from data for triplicate wells. The value was normalized by Renilla luciferase activity. All experiments were repeated at least three times with nearly identical results. Data are expressed as means±S.D. ($n$=3).

**Experiment for the Effects of Test Compounds on NF-$\kappa$B Transcriptional Activity** Plasmid-transfected HCT116, RKO and SW480 cells were cultured in the presence of 25 ng/mL TNF$\alpha$ for 2 or 6 h after 30 min incubation with 25, 50, 100 $\mu$M SK-1009. Similarly, 5HPP-33 (25, 50 $\mu$M), SM-7368 (25, 50 $\mu$M), catechin (100 $\mu$M), dexamethasone (10 $\mu$M) and troglitazone (10 $\mu$M) were added to the medium 30 min before TNF$\alpha$ stimulation. NF-$\kappa$B transcriptional activity was normalized for transfection rate calculated by SV40 promoter driven Renilla luciferase.

**Immunofluorescence Analysis in Cells** HCT116, RKO and SW480 cells were seeded at a density of $8\times10^4$/well in 8-chamber slides, and incubated in the presence or absence of 25 $\mu$g/mL TNF$\alpha$ for 30 min after 30 min pretreatment with or without 50 $\mu$M SK-1009. After incubation, cells were fixed with 2% paraformaldehyde for 30 min at room temprature and permeabilized with methanol for 10 min at −20°C. Cells were subjected to immunofluorescence analysis with anti-NF-$\kappa$B (p65) antibodies (Santa Cruz Biotechnology Inc., Santa Cruz, CA, U.S.A.) at 1 : 100 dilutions followed by anti-rabbit immunoglobulin G (IgG) fluorescein isothiocyanate (FITC) conjugated antibody (Biotium, Hayward, CA, U.S.A.).

**Sodium Dodecyl Sulfate-Polyacrylamide Gel Electrophoresis (SDS-PAGE) and Western Blot Analysis** The cells were lysed in SDS sample buffer solution (62.5 mM Tris–HCl, pH 6.8, 2% SDS, 5% 2-mercaptoethanol, 10% glycerol) and the lysates were briefly sonicated and boiled for 5 min. Proteins from lysates of HCT116, RKO and SW480 cells were separated on polyacrylamide gels and electrophoretically transferred to Immobilon-P membranes (Merck Millipore, Billerica, MA, U.S.A.). After blocking with 2% non-fat skim milk in TTBS (10 mM Tris–HCl, pH 7.5, 140 mM NaCl, 0.05% Tween 20) for 1 h the membranes were incubated with primary antibody in TTBS containing 1% bovine serum albumin, washed with TTBS and incubated with the second antibody, horseradish peroxidase-conjugated anti-rabbit or anti-mouse IgG (Amersham Bioscience, Little Chalfont, U.K.). After further washing with TTBS the blots were developed using an ECL detection kit (GE Healthcare, Little Chalfont, U.K.) and exposed to Kodak XAR-5 film (Eastman Kodak Co., Rochester, NY, U.S.A.). The antibodies were stripped by placing the blots in boiling water for several minutes and then the blots were re-probed with further antibodies: mouse monoclonal anti-$\beta$ actin (Sigma Life Science, St Louis, MO, U.S.A.) and rabbit polyclonal anti-I-$\kappa$B$\alpha$ antibody (Santa Cruz Biotechnology Inc.).

**Transcriptional Factor Activation Profiling Analysis** Activation of several receptors, such as androgen receptor (AR), constitutive active/androstane receptor (CAR), estrogen receptor (ER), glucocorticoid receptor (GR), hepatocyte nuclear factor-4 (HNF4), peroxisome proliferator-activated receptor (PPAR) and pregnane X receptor (PXR) by SK-1009 in HCT-116 cells were evaluated using Transcriptional Factor Activation Profiling Array (Signosis, Inc., Sunnyvale, CA, U.S.A.). HCT116 cells ($3\times10^6$ cells/well) were cultured with or without 50 $\mu$M SK-1009 for 6 h, and then nuclear extracts were obtained by a Nuclear/Cytsol Fraction Kit (BioVision, Milpitas, CA, U.S.A.). Nuclear extracts were incubated with consensus sequences of nuclear receptor DNA-binding sites for determination of transcriptional activities according to the manufacturer's protocol.

**Statistical Analysis** All the results are expressed as mean±S.D. values, with statistical analysis using Bonferroni $z$-test. Differences were considered to be statistically significant at $p<0.05$.

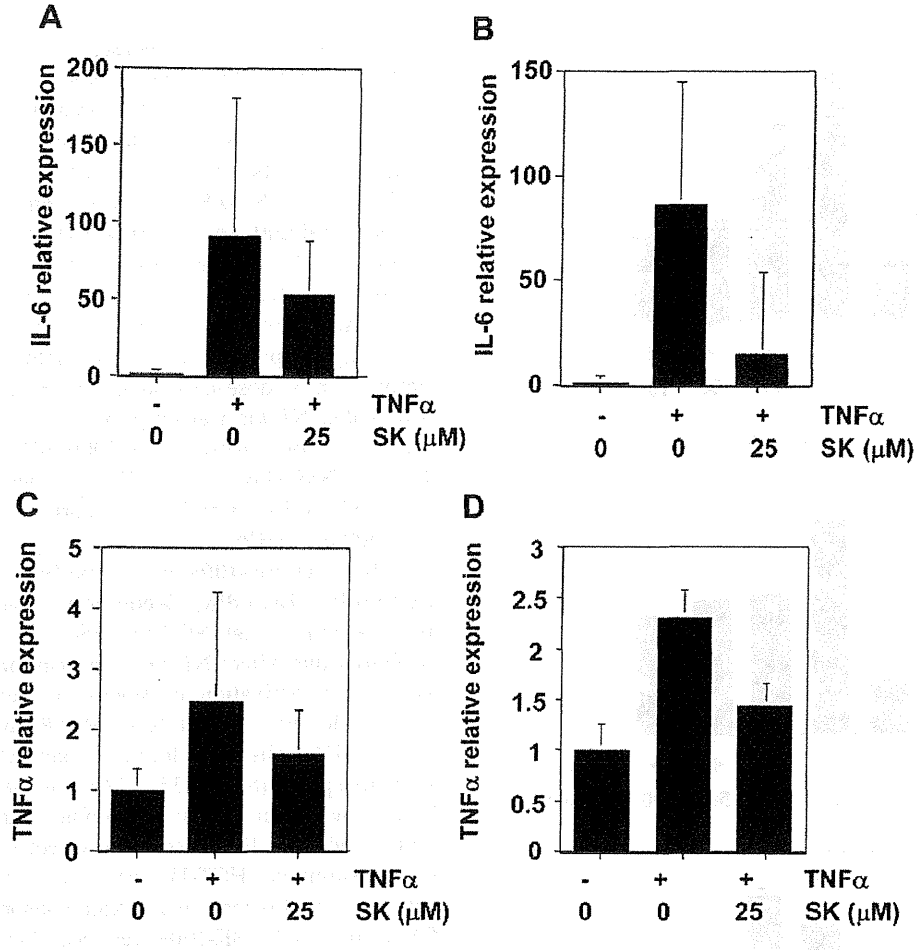


Fig. 2. Effects of SK-1009 on Various Cytokine mRNA Levels

HCT116 (A, C) and RKO (B, D) cells were cultured with and without 25 ng/mL TNFα for 6 h after 30 min incubation with 25 μM SK-1009 (SK). Relative IL-6 (A, B) and TNFα (C, D) mRNA expression levels are plotted as the ratio of the unstimulated control culture value. Data are means±S.D. ($n$=3). Similar results were obtained from more than three separate experiments.

## RESULTS

**Suppression of Cytokine Expression by SK-1009 in TNFα-Stimulated Human Colon Cancer Cells** To confirm that SK-1009 suppresses IL-6 expression levels in colon epithelial cells, HCT116 and RKO cells were stimulated with 25 ng/mL TNFα to induce IL-6 and TNFα mRNA and simultaneously incubated with 25 μM SK-1009. As shown in Fig. 2, SK-1009 treatment suppressed IL-6 and TNFα mRNA levels in TNFα-stimulated cells.

**Inhibition of TNFα-Treated NF-κB Transcriptional Activity by SK-1009 in Human Colon Cancer Cells** NF-κB is the major transcriptional factor responsible for induction of *IL-6* gene expression induced by LPS and inflammatory cytokines. Thus, we assumed that the one of the targets of SK-1009 is NF-κB, and examined the effects of SK-1009 on TNFα-activated NF-κB transcriptional activity using luciferase reporter gene assay. No significant difference was observed in the basal NF-κB transcriptional activity of HCT116 cells between serum-deprived cultures and 5% fetal bovine serum (FBS)-supplemented cultures after 6 h. To examine the effective dose and timing of TNFα, cells were cultured in a medium containing 5, 25 and 100 ng/mL TNFα without FBS, and NF-κB transcriptional activity were tested. Treatment of HCT116 cells with 5, 25 and 100 ng/mL TNFα for 6 h increased the activity to almost 7, 12 and 13 times of the control value, respectively (Suppl. Fig. 1A). NF-κB transcriptional activities after 6 h treatment with TNFα were elevated compared to those of 2 h TNFα treatment in RKO cells and SW480 cells (Suppl. Figs. 1B, C). Moreover, TNFα seems to activate NF-κB transcriptional activities to its maximum at the dose of 25 ng/mL (Suppl. Fig. 1). No significant decrease of cell viability, evaluated by MTT assay, was observed after 6 h culture with TNFα at these concentrations.

The effects of SK-1009 on TNFα-stimulated NF-κB transcriptional activity were next examined, and revealed that SK-1009 significantly suppressed TNFα-stimulated NF-κB transcriptional activity in a dose-dependent manner (Fig. 3). Decreases in TNFα-stimulated NF-κB transcriptional activity at the highest doses of SK-1009 were as follows; 64% for HCT116 cells, 42% for RKO cells and 59% for SW 480 cells (Figs. 3A–C). No significant decrease of cell viability, evaluated by Renilla luciferase activity obtained from Renilla Luciferase Assay Systems and MTT assay, was observed after 6 h culture with TNFα plus SK-1009 at these concentrations. MTT assay revealed less than 4% decrease of cell viability in TNFα plus SK-1009 treatment compared with TNFα alone.

**Inhibition of TNFα-Induced NF-κB Nuclear Translocation and Degradation of the Inhibitory Subunit I-κBα by SK-1009 Treatment** Translocation of NF-κB to the

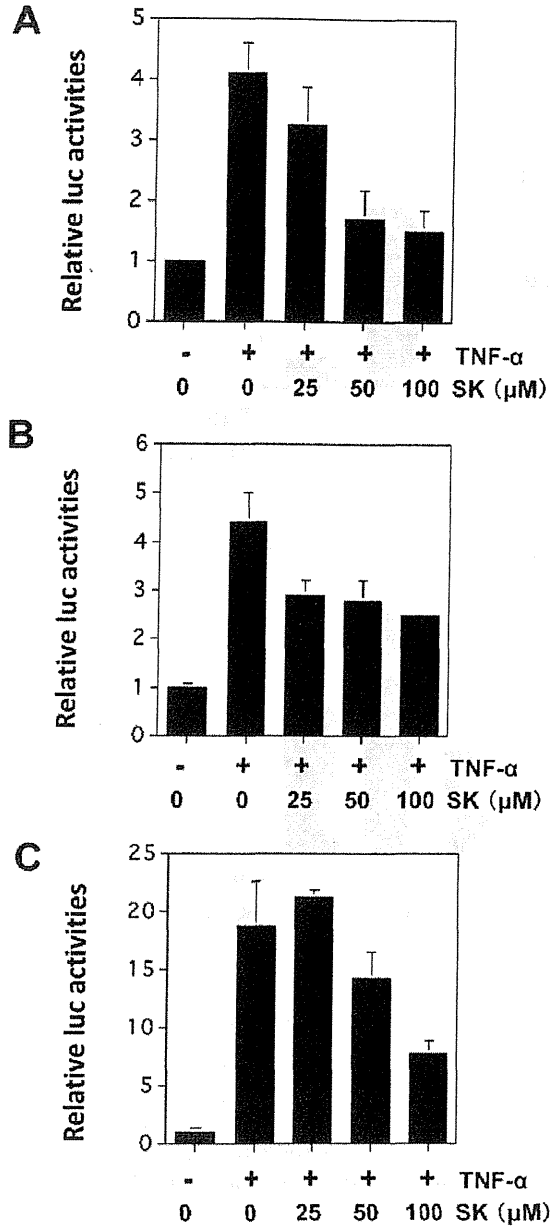


Fig. 3. Effects of SK-1009 on TNFα-Treated NF-κB Transcriptional Activity in Human Colon Cancer Cells

HCT116 (A), RKO (B) and SW480 (C) cells were cultured in the presence of 25 ng/mL TNFα for 6 h after 30 min incubation with the indicated dose of SK-1009. Relative NF-κB transcriptional activities are plotted as the ratio of the unstimulated control culture value. Data are means±S.D. ($n$=3). Similar results were obtained from three separate experiments.

nucleus activates transcription of NF-κB-responsive genes. Thus, we performed fluorescent immunohistochemical analysis of NF-κB subcellular localizations after TNFα treatment in HCT116 cells. TNFα caused NF-κB nuclear translocation within 30 min (Figs. 4A–C) and this was prevented by 50 μM SK-1009 pretreatment for 30 min. Similar results were obtained in SW480 cells, but failed in RKO cells (data not shown).

Translocation of NF-κB to the nucleus is preceded by phosphorylation and proteolytic degradation of the inhibitory subunit I-κBα. To determine whether the effect of SK-1009 on NF-κB activation is related to I-κBα degradation, the I-κBα protein level was examined by Western blot analysis. As shown in Fig. 4D, stimulation of the HCT116 cells with I-κBα caused a rapid decrease in the abundance of I-κBα protein, which almost completely disappeared in stimulated cells 10–30 min after I-κBα stimulation. Similar results were obtained in SW480 cells (data not shown). However, I-κBα degradation was weakly observed in RKO cells (Fig. 4E).

**Effects of NF-κB Inhibitors on TNFα-Treated NF-κB Transcriptional Activity in HT116 Cells** The effects of the available NF-κB inhibitors on TNF-stimulated NF-κB transcriptional activity were examined for the comparison of their potential to those of SK-1009. All the NF-κB inhibitors significantly suppressed TNFα-stimulated NF-κB transcriptional activity in a dose-dependent manner. Decreases in TNFα-stimulated NF-κB transcriptional activity at a dose of 50 μM were as follows; 67% for SK-1009, 65% for 5HPP-33 and 96% for SM-7368 (Fig. 5). SM-7368 showed the strongest inhibition and similar inhibitory potential were observed between SK-1009 and 5HPP-33.

**Effects of SK-1009 on Activation of Nuclear Receptor Subfamily, Including Xenobiotic Receptors** To examine the possibility that SK-1009 could be the ligand for other receptors that affect NF-κB transcriptional activity, we evaluated direct activation of several nuclear receptors, such as AR, CAR, ER, GR, HNF4, PPAR and PXR by SK-1009 in HCT-116 cells, and found no activation was observed in such receptors (Suppl. Fig. 2A). Furthermore, the effects of several agents that regulate xenobiotic metabolism, on TNFα-stimulated NF-κB transcriptional activity in HCT-116 cells were examined. HCT-116 cells were treated with SK-1009 catechin, troglitazone and dexamethasone for 2 h, and it was found that only SK-1009 reduced TNFα-stimulated NF-κB transcriptional activity (Suppl. Fig. 2B). After 6 h, dexamethasone tend to reduce TNFα-stimulated NF-κB transcriptional activity (data not shown). These data demonstrated that the effects of SK-1009 on NF-κB transcriptional activity is faster than that of dexamethasone, and suggested that the effect of SK-1009 is not the result of activation of xenobiotic receptor, such as pregnane X receptor.

## DISCUSSION

The present study demonstrated that SK-1009 significantly suppresses *IL-6* expression levels not only in human macrophage cells, but also in human colon cancer cells stimulated with TNFα. Moreover, we demonstrated clear suppression of activation of transcription factor NF-κB, which has important roles in *IL-6* gene expression with SK-1009 treatment.

Many kinds of transcription factors are known to be involved in transcriptional induction of the *IL-6* gene, such as NF-κB and NF-IL6. Of these, NF-κB is the major transcription factor responsible for induction of the *IL-6* gene expression by LPS and inflammatory cytokines.[13–15] The NF-κB binding site located between -72 and -63 on the *IL-6* gene promoter region is important for IL-6 induction.[16–18] Both p50 and p65 can bind strongly to the κB-like motif of the *IL-6* gene. IL-6 promoter-luciferase reporter gene assay with a site-directed mutant revealed that both NF-IL6 and NF-κB binding sites in the *IL-6* gene are required for the synergistic activation.[19] Thus, we speculated that SK-1009 has the potential to inhibit NF-κB transcriptional activity. In addition, SK-1009 suppressed the expression of several inflammation-related genes including

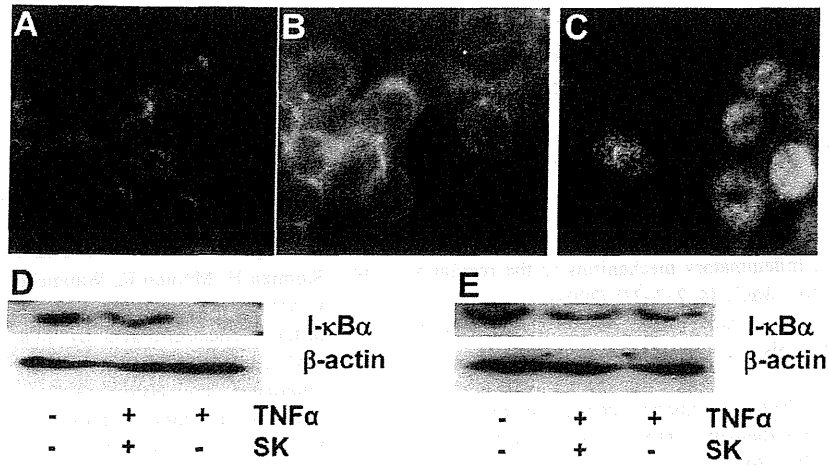


Fig. 4. Effects of SK-1009 on Nuclear Translocation of NF-κB and I-kBα Degradation

HCT116 cells were pre-treated with 50 μM SK-1009, and then 25 ng/mL TNFα were treated with for 30 min. After treatment, cells were fixed with 2% paraformaldehyde and fluorescent immunohistochemical analysis of NF-κB was performed. Control un-treated cells (A), SK-1009 plus TNFα treated cells (B) and TNFα treated cells (C). The data shown are representative of two independent experiments. Western blot analysis of I-κBα protein levels after 0 and 30 min incubation with 25 ng/mL TNFα with or without 50 μM SK-1009 in HCT116 cells (D) and RKO cells (E). Cell lysate proteins were separated on a 15% SDS-polyacrylamide gel. The data shown are representative of two independent experiments.

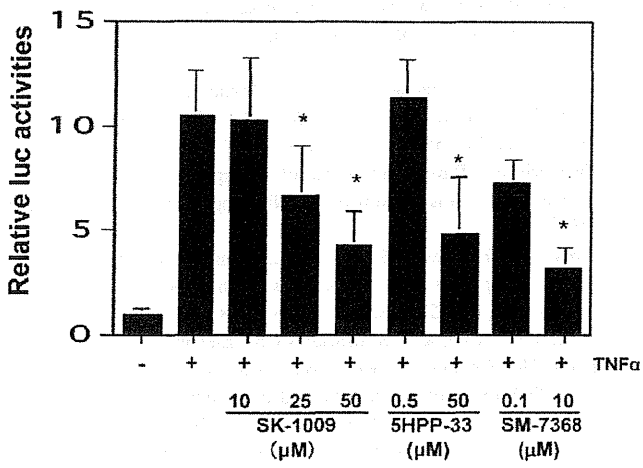


Fig. 5. Effects of NF-κB Inhibitors on TNFα-Treated NF-κB Transcriptional Activity in HCT116 Cells

HCT116 cells were cultured in the presence of 25 ng/mL TNFα for 6 h after 30 min incubation with the indicated dose of NF-κB inhibitors, 5HPP-33 or SM-7368. Relative NF-κB transcriptional activities are plotted as the percentage of the unstimulated control culture value. Data are means±S.D. ($n$=3). *$p$<0.05 *vs.* TNFα treatment. Similar results were obtained from two separate experiments.

cytokines, such as TNFα and IL-8 (data not shown), in which NF-κB plays an important role in its induction. These results support the data that NF-κB could be the target of SK-1009. Meanwhile, not all the IL-6 suppressive effect can't be explained by reduction of NF-κB transcriptional activity, such as that which was observed in RKO cells. We also examined the effects of nuclear receptor activation by SK-1009, but did not obtain data suggesting cross talk between NF-κB transcriptional activity and such nuclear receptors as far as we could find. Further detailed mechanisms underlying suppression of NF-κB transcriptional activity by SK-1009 should be examined in the future.

The importance of NF-κB is demonstrated by its critical role in responses leading to host defense through rapid induction of several genes, such as inflammatory and immunological responses.[20,21] Dysregulation of NF-κB has been linked to pathological dysregulation of various conditions, including inflammatory reactions, septicshock, acquired immunodeficiency syndrome and cancer.[20,21] The NF-κB protein exists in the cytoplasm in an inactive state with an inhibitory subunit I-κBα. Phosphorylation of residues Ser32 and Ser36 of I-κBα and its subsequent degradation allows nuclear translocation of NF-κB. Translocation of NF-κB to the nucleus activates transcription of NF-κB responsive genes,[22,23] such as IL-6 and TNFα. Thus, inhibition of NF-κB by SK-1009 was suggested to be, at least in part, due to inhibition of degradation of I-κBα (Fig. 4). Roles for reactive oxygenspecies, protein kinases, protein phosphatases, proteases and ceramide have been documented in the pathway of I-κBα degradation and NF-κB activation.[20,21] SK-1009 is so novel a compound that the effects on such reactive oxygenspecies production, activation of protein kinases, protein phosphatases, proteases and ceramide are not known yet. Further studies need to be carried out to elucidate the effects of SK-1009 on the pathway of inhibition of degradation of I-κBα.

Evidence is now accumulating that excessive production of IL-6 is a causative factor for carcinogenesis.[24–27] Dysregulated activation of NF-κB has also been suggested to be related to promotion of carcinogenesis.[20,21] Therefore, SK-1009 inhibition of IL-6 production may be causally related to its anticarcinogenic potential. However, it should be borne in mind that NF-κB activity also plays an important role in the immune system. Therefore, it is possible that pronounced inhibition of IL-6 production and transcription factor activities in macrophages and lymphocytes may cause adverse effects, such as immunosuppression and deterioration of the defense system of the host, which may facilitate tumor growth. In order to clarify the applicability of SK-1009 as a cancer preventive agent, animal experiments are now under investigation. Our results have shown an additional candidate NF-κB inhibitor, which could be a cancer preventive agent.

**Acknowledgements** This work was supported by Grants-in-Aid for Cancer Research, for the Third-Term Comprehensive 10-Year Strategy for Cancer Control from the Ministry of Health, Labour, and Welfare of Japan, and also from the Yakult Bio-science Foundation.

## REFERENCES

1) Tilg H, Moschen AR. Inflammatory mechanisms in the regulation of insulin resistance. *Mol. Med.*, **14**, 222–231 (2008).
2) Ishihara K, Hirano T. IL-6 in autoimmune disease and chronic inflammatory proliferative disease. *Cytokine Growth Factor Rev.*, **13**, 357–368 (2002).
3) Oshima H, Oshima M. The inflammatory network in the gastrointestinal tumor microenvironment: lessons from mouse models. *J. Gastroenterol.*, **47**, 97–106 (2012).
4) Mroczko B, Groblewska M, Gryko M, Kedra B, Szmitkowski M. Diagnostic usefulness of serum interleukin 6 (IL-6) and C-reactive protein (CRP) in the differentiation between pancreatic cancer and chronic pancreatitis. *J. Clin. Lab. Anal.*, **24**, 256–261 (2010).
5) Fuksiewicz M, Kowalska M, Kotowicz B, Rubach M, Chechlinska M, Pienkowski T, Kaminska J. Serum soluble tumour necrosis factor receptor type I concentrations independently predict prognosis in patients with breast cancer. *Clin. Chem. Lab. Med.*, **48**, 1481–1486 (2010).
6) Biggar RJ, Johansen JS, Smedby KE, Rostgaard K, Chang ET, Adami HO, Glimelius B, Molin D, Hamilton-Dutoit S, Melbye M, Hjalgrim H. Serum YKL-40 and interleukin 6 levels in Hodgkin lymphoma. *Clin. Cancer Res.*, **14**, 6974–6978 (2008).
7) Sharma R, Zucknick M, London R, Kacevska M, Liddle C, Clarke SJ. Systemic inflammatory response predicts prognosis in patients with advanced-stage colorectal cancer. *Clin. Colorectal Cancer*, **7**, 331–337 (2008).
8) Lutgendorf SK, Weinrib AZ, Penedo F, Russell D, DeGeest K, Costanzo ES, Henderson PJ, Sephton SE, Rohleder N, Lucci JA 3rd, Cole S, Sood AK, Lubaroff DM. Interleukin-6, cortisol, and depressive symptoms in ovarian cancer patients. *J. Clin. Oncol.*, **26**, 4820–4827 (2008).
9) Baltgalvis KA, Berger FG, Pena MM, Davis JM, Muga SJ, Carson JA. Interleukin-6 and cachexia in ApcMin/+ mice. *Am. J. Physiol. Regul. Integr. Comp. Physiol.*, **294**, R393–R401 (2008).
10) Teraoka N, Mutoh M, Takasu S, Ueno T, Yamamoto M, Sugimura T, Wakabayashi K. Inhibition of intestinal polyp formation by pitavastatin, a HMG-CoA reductase inhibitor. *Cancer Prev. Res.* (Phila.), **4**, 445–453 (2011).
11) Barton BE. Interleukin-6 and new strategies for the treatment of cancer, hyperproliferative diseases and paraneoplastic syndromes. *Expert Opin. Ther. Targets*, **9**, 737–752 (2005).
12) Smolen JS, Maini RN. Interleukin-6: a new therapeutic target. *Arthritis Res. Ther.*, **8** (Suppl. 2), S5 (2006).
13) Xie QW, Whisnant R, Nathan C. Promoter of the mouse gene encoding calcium-independent nitric oxide synthase confers inducibility by interferon gamma and bacterial lipopolysaccharide. *J. Exp. Med.*, **177**, 1779–1784 (1993).
14) Xie QW, Kashiwabara Y, Nathan C. Role of transcription factor NF-kappaB/Rel in induction of nitric oxide synthase. *J. Biol. Chem.*, **269**, 4705–4708 (1994).
15) Gao J, Morrison DC, Parmely TJ, Russell SW, Murphy WJ. An interferon-gamma-activated site (GAS) is necessary for full expression of the mouse iNOS gene in response to interferon-gamma and lipopolysaccharide. *J. Biol. Chem.*, **272**, 1226–1230 (1997).
16) Shimizu H, Mitomo K, Watanabe T, Okamoto S, Yamamoto K. Involvement of a NF-kappaB-like transcription factor in the activation of the interleukin-6 gene by inflammatory lymphokines. *Mol. Cell. Biol.*, **10**, 561–568 (1990).
17) Libermann TA, Baltimore D. Activation of interleukin-6 gene expression through the NF-kappaB transcription factor. *Mol. Cell. Biol.*, **10**, 2327–2334 (1990).
18) Zhang YH, Lin JX, Vilcek J. Interleukin-6 induction by tumor necrosis factor and interleukin-1 in human fibroblasts involves activation of a nuclear factor binding to a kappaB-like sequence. *Mol. Cell. Biol.*, **10**, 3818–3823 (1990).
19) Matsusaka T, Fujikawa K, Nishio Y, Mukaida N, Matsushima K, Kishimoto T, Akira S. Transcription factors NF-IL6 and NF-kappa B synergistically activate transcription of the inflammatory cytokines, interleukin 6 and interleukin 8. *Proc. Natl. Acad. Sci. U.S.A.*, **90**, 10193–10197 (1993).
20) Barnes PJ, Karin M. Nuclear factor-kappaB: a pivotal transcription factor in chronic inflammatory diseases. *N. Engl. J. Med.*, **336**, 1066–1071 (1997).
21) Siebenlist U, Franzoso G, Brown K. Structure, regulation and function of NF-κB. *Annu. Rev. Cell Biol.*, **10**, 405–455 (1994).
22) Henkel T, Machleidt T, Alkalay I, Krönke M, Ben-Neriah Y, Baeuerle PA. Rapid proteolysis of I kappaB-alpha is necessary for activation of transcription factor NF-kappaB. *Nature*, **365**, 182–185 (1993).
23) Brown K, Gerstberger S, Carlson L, Franzoso G, Siebenlist U. Control of I kappa B-alpha proteolysis by site-specific, signal-induced phosphorylation. *Science*, **267**, 1485–1488 (1995).
24) Wink DA, Kasprzak KS, Maragos CM, Elespuru RK, Misra M, Dunams TM, Cebula TA, Koch WH, Andrews AW, Allen JS, Keefer LK. DNA deaminating ability and genotoxicity of nitric oxide and its progenitors. *Science*, **254**, 1001–1003 (1991).
25) Liu RH, Jacob JR, Hotchkiss JH, Cote PJ, Gerin JL, Tennant BC. Woodchuck hepatitis virus surface antigen induces nitric oxide synthesis in hepatocytes: possible role in hepatocarcinogenesis. *Carcinogenesis*, **15**, 2875–2877 (1994).
26) Ohshima H, Bartsch H. Chronic infections and inflammatory processes as cancer risk factors: possible role of nitric oxide in carcinogenesis. *Mutat. Res.*, **305**, 253–264 (1994).
27) Haswell-Elkins MR, Satarug S, Tsuda M, Mairiang E, Esumi H, Sithithaworn P, Mairiang P, Saitoh M, Yongvanit P, Elkins DB. Liver fluke infection and cholangiocarcinoma: model of endogenous nitric oxide and extragastric nitrosation in human carcinogenesis. *Mutat. Res.*, **305**, 241–252 (1994).

## RESULTS

Three-dimensional surface-rendered images of intercalated duct cells, centroacinar cells, and pancreatic ductular systems in the rat pancreas are shown in Figure 1B and C. The point of view in Figure 1C (translucent image) is rotated 140 degrees from that in Figure 1B using the intercalated duct as the axis. The intercalated duct lumen (black arrow in Fig. 1C) was formed by the apical surfaces of only 3 intercalated duct cells, each of which was connected to the centroacinar cells of both acini. The apical surfaces of acinar cells formed the central lumina along with the basolateral surfaces of intercalated duct cells (light blue arrows in Fig. 1B and C), as well as the centroacinar cells (green arrows in Fig. 1B and C). The central lumen entered the depression of the basal surface on the intercalated duct (white arrow in Fig. 1B and D) and joined the intercalated duct lumen (black arrow in Fig. 1E). Figure 1F shows a traced TEM photograph of the part corresponding to the depression on the basal surface of the intercalated duct indicated by white arrows in Figure 1D and E, which revealed that this depression corresponded to the wedged in part of the acinar cell. Light microscopic examinations of the 50 serial semithin sections (1.0 μm thick) before and after obtaining the 101 serial ultrathin sections demonstrated blind alleys of acini in the lower portion of Figure 1A and connection of the centroacinar cells in the upper portion of Figure 1A with the larger intralobular duct.

## DISCUSSION

We were able to clarify the fine 3D structure of the peripheral exocrine gland in the rat pancreas using TEM examinations of 101 serial sections from a pancreatic tissue specimen. Figure 1G presents a schematic representation of the peripheral exocrine gland in the rat pancreas based on the results of our presents and previous studies.[5–9] On the basis of our findings, we made the following conclusions. (1) One or more acinar cells with central lumina are wedged among the intercalated duct cells and face the intercalated duct lumen. (2) Acinar cells adjoining these wedged acinar cells cover the intercalated duct and form the acinus. Not all acini are formed at the ends of the intercalated ducts. (3) The apical surfaces of acinar cells form the central lumina along with the basolateral surfaces of intercalated duct cells, as well as their apical surfaces. (4) Centroacinar cells are intercalated duct cells that have become wedged in and covered by acinar cells.

## ACKNOWLEDGMENTS

*The authors thank Ms Yuko Okui and Mr Tsunao Yoneyama for the technical assistance.*

*The authors declare no conflict of interest.*

**Nobuo Ashizawa, MD, PhD**
Division of Gastroenterology, Tamatsukuri Kousei-Nenkin Hospital, Matsue, Japan
ashizawa.n@smn.enjoy.ne.jp

**Yoshikazu Kinoshita, MD, PhD**
Division of Internal Medicine Second Unit, Shimane University, Izumo, Japan

## REFERENCES

1. Inada A, Nienaber C, Katsuta H, et al. Carbonic anhydrase II-positive pancreatic cells are progenitors for both endocrine and exocrine pancreas after birth. *Proc Natl Acad Sci U S A.* 2008;105:19915–19919.
2. Furuyama K, Kawaguchi Y, Akiyama H, et al. Continuous cell supply from a Sox9-expressing progenitor zone in adult liver, exocrine pancreas and intestine. *Nat Genet.* 2011;43:34–41.
3. Bockman DE. Anastomosing tubular arrangement of the exocrine pancreas. *Am J Anat.* 1976;147:113–118.
4. Takahashi H. Scanning electron microscopy of the rat exocrine pancreas. *Arch Histol Jpn.* 1984;47:387–404.
5. Ashizawa N, Sakai T, Yoneyama T, et al. Three-dimensional structure of peripheral exocrine gland in rat pancreas. *Pancreas.* 2005;31:401–404.
6. Ashizawa N, Watanabe M, Fukumoto S, et al. Scanning electron microscopic observation of three-dimensional structure of the rat pancreatic duct. *Pancreas.* 1991;5:542–550.
7. Ashizawa N, Endo H, Hidaka K, et al. Three-dimensional structure of the rat pancreatic duct in normal and inflammated pancreas. *Microsc Res Tech.* 1997;37:543–556.
8. Endo H, Ashizawa N, Niigaki Ma, et al. Fine reconstruction of the pancreatic ductular system at the onset of pancreatitis. *Histol Histopathol.* 2002;17:107–112.
9. Ashizawa N, Hamamoto N, Endo H, et al. The fine structure of rat pancreatic duct system [in Japanese]. *J Jpn Panc Soc.* 2004;19:23–32.

# Invasive Ductal Carcinoma Developing in Pancreas With Severe Fatty Infiltration

***To the Editor:***

The pathogenesis of fatty pancreas, characterized by massive infiltration of adipocytes into the pancreatic tissue, is still unclear, as is the association of fatty infiltration with neoplastic lesions. We report a 69-year-old man who was admitted for evaluation of a pancreatic tumor detected by computed tomography (CT) during a routine follow-up examination. Nine years previously, he had undergone distal gastrectomy for early gastric cancer. A CT scan 5 years before admission had shown replacement of most of the pancreas with fat tissue. Pretreatment CT demonstrated an irregularly demarcated pancreatic head tumor with dilatation of the upstream main pancreatic duct within the surrounding pancreatic tissue, which continued to show fatty replacement. Analysis of the pancreatoduodenectomy specimen revealed that tubular adenocarcinoma had proliferated in the head of the pancreas, most of which had been markedly infiltrated by adipose tissue. To our knowledge, this is the first report to have documented the development of pancreatic head carcinoma in a pancreas background showing total fat replacement.

## CASE REPORT

A 69-year-old man was admitted for evaluation of a pancreatic tumor detected by CT during a routine follow-up examination. He had undergone distal gastrectomy for early gastric cancer 9 years previously when his body mass index had been 27.3. He had no history of pancreatitis, diabetes mellitus, or dyslipidemia. The CT scan 5 years before admission had shown replacement of most of the pancreas with fat tissue (Fig. 1A). Physical examination revealed no organomegaly or a palpable abdominal mass.

Laboratory studies on admission revealed elevated levels of blood glucose (201 mg/dL) and tumor marker (CA 19-9:195 U/mL). Serum lipid levels were normal during the entire follow-up period. Contrast-enhanced CT (Fig. 1B) showed an irregularly demarcated pancreatic head tumor with dilatation of the upstream main pancreatic duct within the surrounding pancreatic tissue, which continued to show fatty replacement.

The patient underwent pancreatoduodenectomy under a clinical diagnosis of pancreatic cancer. Pathological examination showed that ductal adenocarcinoma had proliferated in the pancreas head (Fig. 1C) and formed a 30-mm irregularly shaped tumor that had infiltrated into the surrounding connective tissues, mesocolon, and superior mesenteric vein. This moderately differentiated tubular adenocarcinoma had not metastasized to the regional lymph nodes. Adipose tissue had markedly infiltrated the noncancerous pancreatic tissue

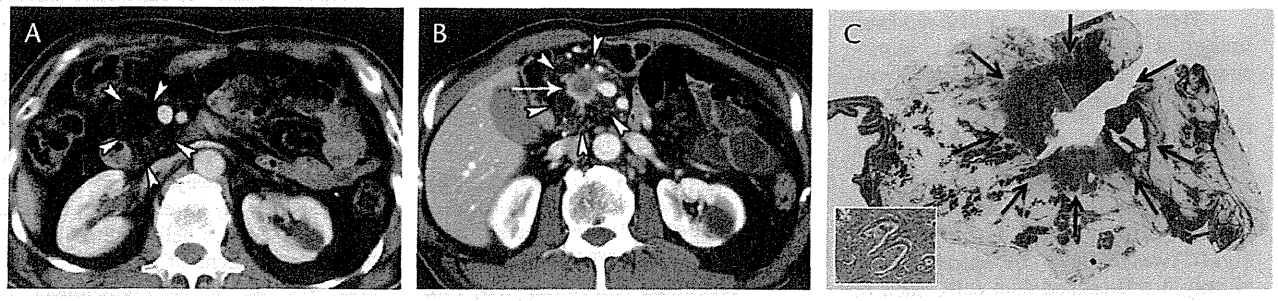


**FIGURE 1.** A, A CT image obtained 5 years before detection of the pancreatic cancer, showing severe fatty infiltration of the pancreas (arrowheads). B, The CT on admission showing a hypoattenuating tumor (arrow) in the pancreas with fatty replacement (arrowheads). C, Histological examination of a resected specimen showing tubular adenocarcinoma (arrows) within the pancreas markedly replaced by fat tissue (loupe view). Carcinoma cells proliferating with a tubular growth pattern and infiltrating into dense fibrous tissue (inset, high-power view).

and replaced most of the pancreatic parenchyma. The CT examination 3 months after the operation revealed suspected lymph node metastasis, and the patient received chemotherapy. At 45 months after surgery, the patient died because of progression of the disease.

## DISCUSSION

Age, obesity, and diabetes mellitus are considered to be the etiological factors related to fatty infiltration of the pancreas and are also suggested to be the risk factors for pancreatic cancer.[1,2] A few cases of pancreatic tumors other than ductal adenocarcinoma have been reportedly associated with pancreatic fatty infiltration.[3–6] However, because no information about the state of the pancreas before tumor development was available for any of these cases, it is unclear whether fatty infiltration of the pancreas had been present before tumor formation, or whether fatty infiltration had been induced secondarily by the tumor. In the present case, follow-up by CT examination made it possible to demonstrate the relationship between fatty pancreas and the development of pancreatic cancer.

Pancreatic fatty infiltration often occurs because of obstruction of the pancreatic duct or vasculature for several reasons, and this event has been observed in experimental animal models.[7] Therefore, fatty infiltration in the pancreas can be induced secondarily by development of a tumor, or can also be induced genetically or environmentally.[8,9] Using a hamster model, we have shown that a high-fat diet increases fatty infiltration and the expression of adipocytokines and growth factors in the pancreas, and that the development of carcinogen-induced pancreatic cancer is enhanced, suggesting that factors associated with fatty infiltration may contribute to pancreatic cancer development.[10]

Here, we have described a case of pancreatic head cancer that developed in a pancreas showing marked fatty infiltration, which had been evident on CT images obtained 5 years before detection of the pancreatic cancer. This is the first reported case of invasive ductal carcinoma to have developed in a fatty pancreas that was detected before cancer formation, and our findings suggest that pancreatic cancer may be associated with fatty infiltration and that fatty pancreas could be a feature suggestive of pancreatic cancer risk. Clearly, this case needs to be interpreted carefully, because the infiltration of adipose tissue into the pancreas was exceptionally severe, and it is still unclear whether this case is sufficiently representative of fatty infiltration in the pancreas generally. Further prospective cohort studies will be necessary to clarify whether generalized fatty infiltration into the pancreas could act as a background for development of pancreatic cancer.

## ACKNOWLEDGMENT

*None of the authors received funding from any source in relation to this study.*

*The authors declare no conflict of interest.*

**Mika Hori, PhD**
Division of Cancer Development System
National Cancer Center Research Institute
Tokyo, Japan

**Hiroaki Onaya, MD, PhD**
Diagnostic Radiology Division
National Cancer Center Hospital
Tokyo, Japan

**Mami Takahashi, PhD**
Central Animal Division
National Cancer Center Research Institute
Tokyo, Japan

**Nobuyoshi Hiraoka, MD, PhD**
Division of Molecular Pathology
National Cancer Center Research Institute
Tokyo, Japan

**Michihiro Mutoh, MD, PhD**
Division of Cancer Prevention Research
National Cancer Center Research Institute
Tokyo, Japan

**Tomoo Kosuge, MD, PhD**
Hepatobiliary and Pancreatic Surgery Division
National Cancer Center Hospital, Tokyo, Japan

**Hitoshi Nakagama, MD, PhD**
Division of Cancer Development System
National Cancer Center Research Institute
Tokyo, Japan
hnakagam@ncc.go.jp

## REFERENCES

1. Patel AV, Rodriguez C, Bernstein L, et al. Obesity, recreational physical activity, and risk of pancreatic cancer in a large U.S. cohort. *Cancer Epidemiol Biomarkers Prev.* 2005;14:459–466.
2. Huxley R, Ansary-Moghaddam A, Berrington de González A, et al. Type-II diabetes and pancreatic cancer: a meta-analysis of 36 studies. *Br J Cancer.* 2005;92:2076–2083.
3. Nakamura Y, Egami K, Maeda S, et al. Solid and papillary tumor of the pancreas complicating agenesis of the dorsal pancreas. *J Hepatobiliary Pancreat Surg.* 2001;8:485–489.
4. Cohen DJ, Fagelman D. Pancreas islet cell carcinoma with complete fatty replacement: CT characteristics. *J Comput Assist Tomogr.* 1986;10: 1050–1051.
5. Shimizu M, Hirokawa M, Matsumoto T, et al. Fatty replacement of the pancreatic body and tail associated with leiomyosarcoma of the pancreatic head. *Pathol Int.* 1997;47: 633–636.

6. Eriguchi N, Aoyagi S, Hara M, et al. Insulinoma occurring in association with fatty replacement of unknown etiology in the pancreas: report of a case. *Surg Today.* 2000;30: 937–941.
7. Watanabe S, Abe K, Anbo Y, et al. Changes in the mouse exocrine pancreas after pancreatic duct ligation: a qualitative and quantitative histological study. *Arch Histol Cytol.* 1995;58:365–374.
8. Golson ML, Loomes KM, Oakey R, et al. Ductal malformation and pancreatitis in mice caused by conditional jag1 deletion. *Gastroenterology.* 2009;136:1761–1771.
9. Pinnick KE, Collins SC, Londos C, et al. Pancreatic ectopic fat is characterized by adipocyte infiltration and altered lipid composition. *Obesity.* 2008;16: 522–530.
10. Hori M, Kitahashi T, Imai T, et al. Enhancement of carcinogenesis and fatty infiltration in the pancreas in N-nitrosobis (2-oxopropyl) amine-treated hamsters by high fat diet. *Pancreas.* 2011;40: 1234–1240.